The *RIN-MC* Fusion of MADS-Box Transcription Factors Has Transcriptional Activity and Modulates Expression of Many Ripening Genes[1]

Shan Li,[a,b] Huijinlan Xu,[a] Zheng Ju,[a] Dongyan Cao,[a] Hongliang Zhu,[a] Daqi Fu,[a] Donald Grierson,[c,d] Guozheng Qin,[e] Yunbo Luo,[a,2] and Benzhong Zhu[a,2]

[a]College of Food Science and Nutritional Engineering, China Agricultural University, Beijing 100083, People's Republic of China

[b]Hubei Provincial Research Center of Engineering Technology for Utilization of Botanical Functional Ingredients, Hubei Engineering University, Xiaogan 432000, People's Republic of China

[c]Zhejiang Provincial Key Laboratory of Horticultural Plant Integrative Biology, Zhejiang University, Zijingang Campus, Hangzhou 310058, People's Republic of China

[d]Division of Plant and Crop Sciences, School of Biosciences, University of Nottingham, Sutton Bonington Campus, Loughborough LE12 5RD, United Kingdom

[e]Key Laboratory of Plant Resources, Institute of Botany, Chinese Academy of Sciences, Beijing 100093, People's Republic of China

ORCID IDs: 0000-0002-1484-2212 (H.Z.); 0000-0002-2238-8072 (D.G.); 0000-0003-3046-1177 (G.Q.); 0000-0002-7089-4703 (B.Z.).

Fruit development and ripening is regulated by genetic and environmental factors and is of critical importance for seed dispersal, reproduction, and fruit quality. Tomato (*Solanum lycopersicum*) *ripening inhibitor* (*rin*) mutant fruit have a classic ripening-inhibited phenotype, which is attributed to a genomic DNA deletion resulting in the fusion of two truncated transcription factors, *RIN* and *MC*. In wild-type fruit, RIN, a MADS-box transcription factor, is a key regulator of the ripening gene expression network, with hundreds of gene targets controlling changes in color, flavor, texture, and taste during tomato fruit ripening; *MC*, on the other hand, has low expression in fruit, and the potential functions of the *RIN-MC* fusion gene in ripening remain unclear. Here, overexpression of *RIN-MC* in transgenic wild-type cv Ailsa Craig tomato fruits impaired several ripening processes, and down-regulating *RIN-MC* expression in the *rin* mutant was found to stimulate the normal yellow mutant fruit to produce a weak red color, suggesting a distinct negative role for *RIN-MC* in tomato fruit ripening. By comparative transcriptome analysis of *rin* and *rin 35S::RIN-MC* RNA interference fruits, a total of 1,168 and 1,234 genes were identified as potential targets of RIN-MC activation and inhibition. Furthermore, the *RIN-MC* fusion gene was shown to be translated into a chimeric transcription factor that was localized to the nucleus and was capable of protein interactions with other MADS-box factors. These results indicated that tomato RIN-MC fusion plays a negative role in ripening and encodes a chimeric transcription factor that modulates the expression of many ripening genes, thereby contributing to the *rin* mutant phenotype.

Fruit ripening is a physiological process involving the development of quality attributes such as color, texture, flavor, and aroma that facilitate seed dispersal and generate the nutritional and organoleptic properties valued by humans (Alba et al., 2005; Klee and Giovannoni, 2011). The dramatic changes occurring during this complex developmental process are genetically regulated and also influenced by environmental factors such as temperature and light (Matas et al., 2009) plus internal regulators (Seymour et al., 2008), including hormones, particularly ethylene (Barry and Giovannoni, 2007; Grierson, 2013), transcription factors (Qin et al., 2012), and epigenetic modifications (Zhong et al., 2013). Investigation of a series of ripening-inhibited tomato (*Solanum lycopersicum*) mutants has identified key transcription factors such as *ripening inhibitor* (*rin*; Vrebalov et al., 2002), *colorless nonripening* (*cnr*; Manning et al., 2006), and *nonripening* (*nor*; Giovannoni, 2004), whose disruption results in impaired ripening, and some ethylene response factors (ERFs), which control different facets of the response (Liu et al., 2016).

The characterization of the *rin* mutant led directly to the identification of the RIN MADS-box transcription factor, which plays a central regulating role in tomato fruit ripening (Vrebalov et al., 2002). Based on comparison between wild type cv Ailsa Craig (AC) and *rin* mutant plants,

[1] This work was supported by the National Natural Science Foundation of China (NSFC 31571894 and 31271959) and the Education Foundation of Da Bei Nong Group (1061-2415002).

[2] Address correspondence to lyb@cau.edu.cn and zbz@cau.edu.cn.

The author responsible for distribution of materials integral to the findings presented in this article in accordance with the policy described in the Instructions for Authors (www.plantphysiol.org) is: Benzhong Zhu (zbz@cau.edu.cn).

B.Z. conceived and designed the experiments; S.L. and H.X. performed the experiments; Z.J. and D.C. analyzed the data; H.Z., D.F., and G.Q. provided technical assistance; Y.L. contributed reagents/materials/analysis tools; D.G. edited the article and contributed to the presentation and interpretation of results; S.L. wrote the article.

www.plantphysiol.org/cgi/doi/10.1104/pp.17.01449

the mutation was shown to cause a severely inhibited ripening phenotype, including loss of the characteristic burst of ethylene production and respiratory climacteric normally associated with the onset of ripening and a severe reduction in pigment accumulation, flavor production, and softening (Vrebalov et al., 2002). The *rin* mutation alters the expression of at least 241 genes (Fujisawa et al., 2013) involved in many aspects of ripening-related pathways, such as ethylene synthesis (*ACS2* and *ACS4*; Fujisawa et al., 2013, 2014), cell wall modification (*PG*, *TBG4*, and *EXP1*; Fujisawa et al., 2013), and volatile production (*LoxC*; Qin et al., 2012). Moreover, RIN is involved in epigenetic modification such as DNA methylation, and the global methylation level of *rin* fruit remained higher than in the wild type at the onset of ripening (Zhong et al., 2013). Comparisons of transcriptome, proteome, and metabolome between the *rin* mutant and wild-type fruits have confirmed that RIN is a global regulator of the tomato fruit-ripening process (Osorio et al., 2011).

The *rin* ripening mutation in tomato is caused by the deletion of a genomic DNA fragment on chromosome 5, resulting in the fusion of adjacent truncated *RIN* and *MC* genes (*RIN-MC*), and the ripening-inhibited phenotype is attributed to the lack of a functional RIN protein. It is known that fusions of distinct genetic loci also have the potential to generate novel functions, which can change the phenotype in plants (Long et al., 2003; Hagel and Facchini, 2017). In opium poppy (*Papaver somniferum*), for example, fusion of the *DRS* and *DRR* genes led directly to an abnormal benzylisoquinoline alkaloid biosynthesis pathway (Li et al., 2016; Hagel and Facchini, 2017). Furthermore, in Arabidopsis (*Arabidopsis thaliana*) and rice (*Oryza sativa*), approximately 110 and 45 genes, respectively, could be transcribed as fusion mRNAs resulting potentially in chimeric proteins, which might provide clues to explore intrinsic regulating mechanisms (Shahmuradov et al., 2010). However, although high expression of the *RIN-MC* fusion gene has been detected in *rin* mutant fruit at the ripe stage based on RNA sequencing technology (Zhong et al., 2013; Fujisawa et al., 2014), possible functions of the *RIN-MC* fusion gene in the *rin* mutant are unknown.

In this study, the functions of *RIN-MC* in tomato fruit ripening were identified both in mutant fruit, in which *RIN-MC* was silenced, and in overexpressing wild-type fruit, which had an altered phenotype. RIN-MC was shown to be a new transcriptional factor by nuclear localization of the RIN-MC fusion protein and the demonstration that it could interact with other transcription factors, and *RIN-MC* functions were confirmed by comparative transcriptome analysis of *rin* and *rin 35S::RIN-MC* RNA interference (RNAi) fruits as well as AC and AC *35S::RIN* RNAi fruits.

RESULTS

Transcription and Translation Assay of *RIN-MC* in Tomato Fruit Ripening

Two pairs of primers were designed to analyze *RIN* and *RIN-MC* transcripts in normal (AC) and *rin* mutant tomato fruits. Primer pair 1 mapped to the portion of the truncated *RIN* and primer pair 2 mapped to a specific region of the truncated *MC* present in the *RIN-MC* fusion (Fig. 1A). The reverse transcription-quantitative PCR (RT-qPCR) results showed that *RIN-MC* was expressed at high levels in *rin* fruits at MG (mature green), BK (breaker; the onset of color changes), yellow, and yellow ripe stages compared with normal *RIN* and *MC* genes in wild-type AC fruit (Fig. 1B). In contrast, only a very low level of transcripts from the normal *MC* gene was detected with primer pair 2 in the wild type (AC), in accordance with earlier findings (Vrebalov et al., 2002; Fig. 1B). The data obtained with both primer pairs suggested high abundance of *RIN-MC* transcripts in the *rin* mutant and were entirely consistent with the *RIN-MC* expression pattern reported in recent transcriptome assays of *rin* mutant fruit (Zhong et al., 2013; Fujisawa et al., 2014).

The effects of the ripening hormone ethylene and its competitive inhibitor 1-methylcyclopropene (1-MCP) on the accumulation of *RIN* mRNA in wild-type (AC) fruit and of *RIN-MC* transcripts in *rin* fruit at the MG stage were examined using primer pair 1 (Fig. 1C). Ethylene stimulated the accumulation of *RIN-MC* transcripts, and there was also a small stimulation of *RIN* mRNA. The significance of this is not clear, since both genes have the same promoter, but it may be related to differences in transcript processing, stability, or regulation by upstream factors. The addition of 1-MCP reduced *RIN* transcripts, suggesting that at least part of the increase is a genuine ethylene response, but the small reduction of *RIN-MC* RNA caused by 1-MCP was not statistically significant.

In wild-type (AC) fruit, *RIN* and *MC* encode the MADS-box transcription factors, RIN and MC, which belong to the MIKC class. According to the coding sequence (CDS) of *RIN-MC* (AF448523) in the National Center for Biotechnology Information database, the *RIN-MC* fusion gene could encode a MADS-box protein consisting of the MADS box (M), Intervening (I), keratin-like (K), and a major part of the C-terminal end (C) of RIN and nearly the complete I region, complete K region, and C-terminal end of MC (Fig. 2A). When the RIN-MC fusion protein with an N-terminal Flag-4myc (FM) tag was overexpressed in the *Nicotiana benthamiana* leaf transient expression system, the translation product from the *RIN-MC* gene was detected using anti-myc antibody (Fig. 2B). The potential endogenous RIN-MC chimeric protein also was assayed in *rin* mutant ripening fruits at different stages of development. Previously, it was reported that little or no signal could be detected for RIN-MC chimeric protein using antibody against partial RIN protein in *rin* mutant fruit (Ito et al., 2008; Martel et al., 2011; Qin et al., 2012); therefore, a specific antibody raised against the C-terminal end of RIN-MC (named MC antibody) was used in this study, in order to probe for MC polypeptide sequences in ripening wild-type (AC) fruit. The RIN-MC protein was detected in great abundance at the BK and yellow stages of *rin* fruits, whereas only a small amount of MC protein was found in AC (wild-type) tomato (Fig. 2C). A specific antibody was raised against the partial C-terminal end of RIN

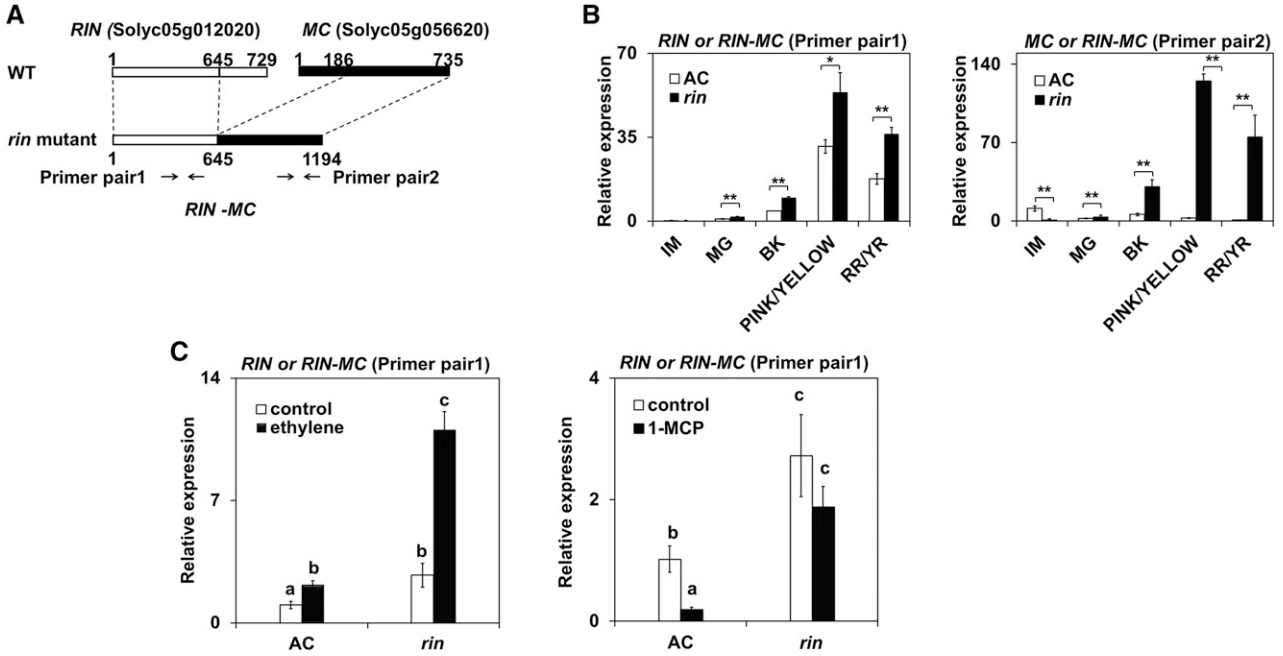

Figure 1. Transcription assay of the *RIN-MC* gene in tomato fruit. A, The expression pattern of the *RIN-MC* gene was measured with different primer pairs, primer pair 1 and primer pair 2, mapped to partial *RIN* and *MC*, respectively, which detect *RIN* or *RIN-MC* (primer pair 1) and *MC* or *RIN-MC* (primer pair 2). WT, Wild type. B and C, Expression was analyzed at various ripening stages in wild-type and *rin* fruit (B) and after treatment with ethylene and 1-MCP at the MG stage (C). Relative transcript levels were determined by RT-qPCR, relative to the expression of the tomato internal control *ACTIN* gene, expressed as $2^{-\Delta\Delta Ct}$ (Livak and Schmittgen, 2001). The stages of fruit ripening are as follows: immature (IM), MG, BK, pink/yellow, and red ripe (RR)/yellow ripe (YR). Relative values were based on comparisons of expression levels at different ripening stages with expression at the IM stage. Asterisks above the bars indicate values with significant differences, which were determined by Student's *t* test (*, $P < 0.05$ and **, $P < 0.01$), and lowercase letters also indicate significant differences.

present in RIN-MC, named RIN-specific antibody, as a probe for the RIN-MC chimeric protein, which was detected at the BK and yellow stages of *rin* mutant tomato fruits (Fig. 2D) and was found with strong signals that indicated its high abundance compared with endogenous RIN protein in wild-type AC fruits. Taken together, this evidence showed that RIN-MC protein accumulates in *rin* mutant fruit and is present in greater abundance at the BK and yellow stages compared with either RIN or MC protein at the corresponding stages in wild-type AC fruits (Fig. 2, C and D); a similar conclusion was published by Ito et al. (2017).

Overexpression of the *RIN-MC* Fusion Gene Inhibits Tomato Fruit Ripening

The function of the *RIN-MC* fusion gene was analyzed by overexpressing it in transgenic wild-type (AC) fruits under the control of the cauliflower mosaic virus (CaMV) 35S promoter (Fig. 3). Overexpression of *RIN-MC* in wild-type fruits resulted in a yellow-colored phenotype at the BK+10 stage (10 d after the start of color change; Fig. 3A). There was no statistically significant difference in *RIN* expression between the wild-type control and transgenic fruits (Fig. 3C), indicating a distinct inhibitory effect of the *RIN-MC* gene or protein on tomato fruit ripening that did not operate by silencing the normal *RIN* gene. Expression of the RIN-MC protein was confirmed in AC::*35S-FM-RIN-MC* fruits by western-blot assay using anti-myc antibody (Fig. 3B), consistent with that observed expressing *FM-RIN-MC* in the leaf transient expression system (Fig. 2B). Several ripening-related genes were down-regulated in the transgenic AC::*35S-FM-RIN-MC* fruits, such as lipoxygenase (*LoxC*), phytoene synthase (*PSY1*), ζ-carotene desaturase (*ZDS*), and polygalacturonase (*PG2a*). Genes related to the ethylene biosynthesis pathway, on the other hand, including ACC synthase (*ACS2* and *ACS4*) and ACC oxidase (*ACO1*), displayed no statistically significant difference between AC and AC::*35S-FM-RIN-MC* fruits (Fig. 3C), indicating that the altered ripening was unlikely to be due to an effect on ethylene synthesis.

Silencing *RIN-MC* Accelerated Yellow Ripening in *rin* Mutant Tomato Fruit

As high expression of the *RIN-MC* fusion gene was detected in *rin* mutant fruits at and after ripening onset (Fig. 1B), the question arises whether it functions in the tomato ripening process. TRV-mediated virus-induced gene silencing (VIGS) was employed as a fast and

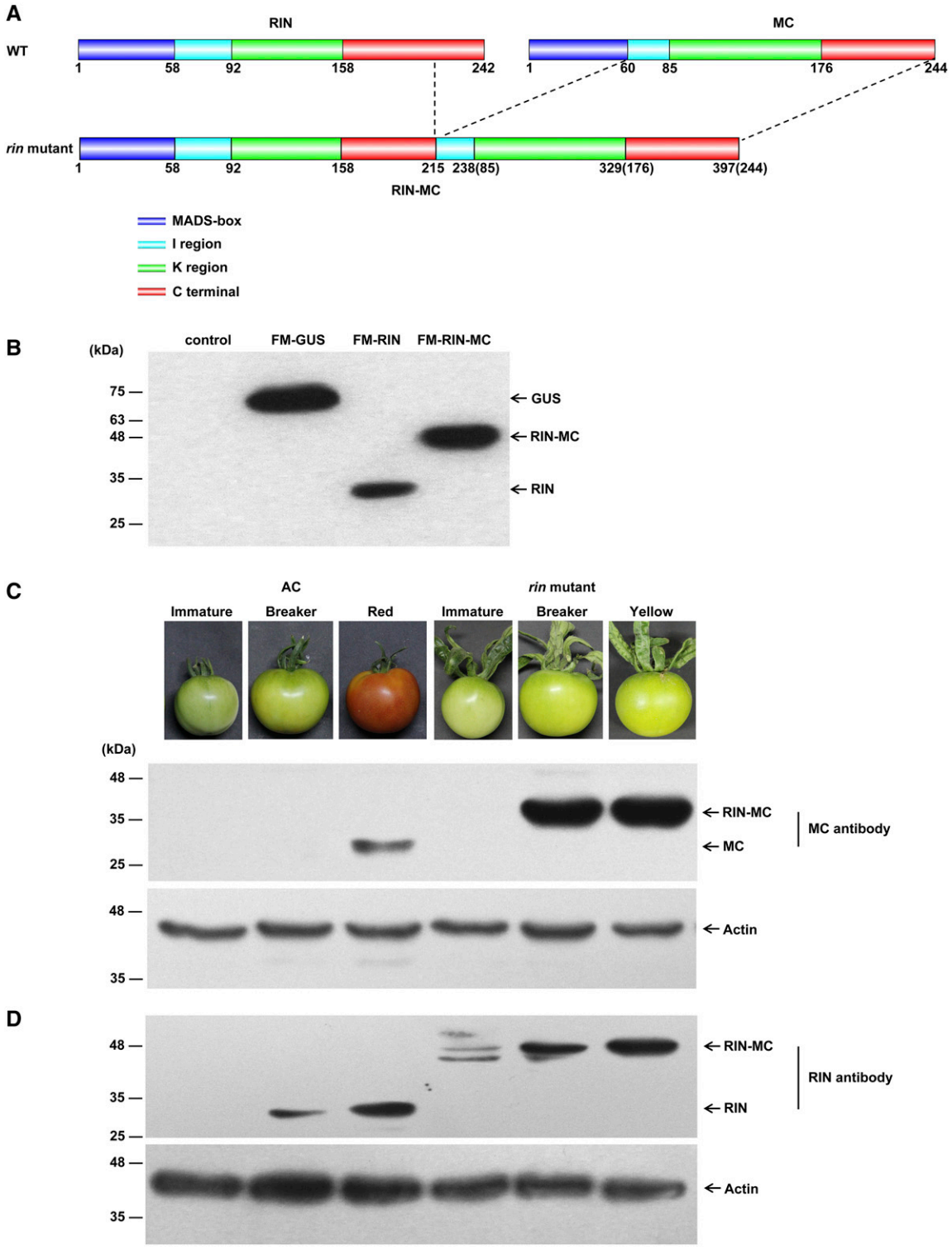

Figure 2. Translation assay of the *RIN-MC* gene in tomato fruit. A, Predicted structure of RIN-MC protein based on its published CDS (AF448523; Vrebalov et al., 2002), visualized in DOG2.0.1 (http://dog.biocuckoo.org/; Ren et al., 2009). WT, Wild type. B, Assay of RIN and RIN-MC protein following transient expression in *N. benthamiana* leaves of FM-GUS, FM-RIN-MC, and FM-RIN. The western blot shows control (expressing empty vector) and experimental constructs using anti-myc antibody. C and D, Endogenous RIN-MC protein in the wild type (AC) and the *rin* mutant at different ripening stages using MC antibody (C) and RIN antibody (D). Actin was used as an internal protein control.

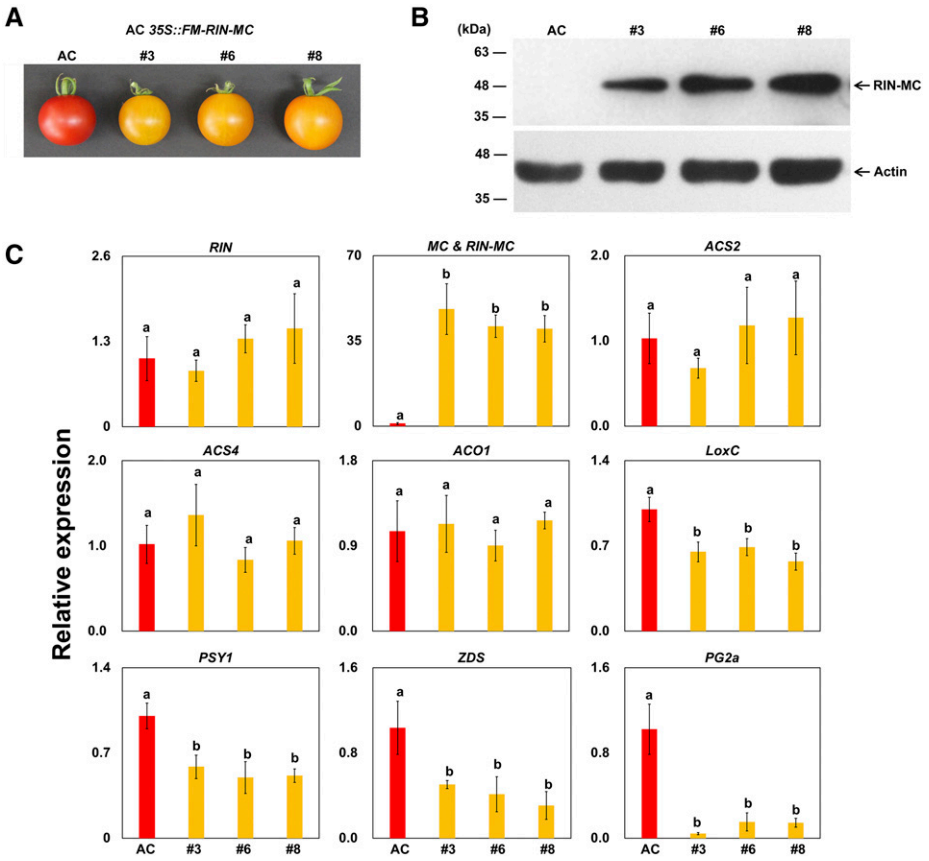

Figure 3. Effects on tomato ripening of the overexpression of RIN-MC in wild-type (AC) fruits. Results from three transgenic lines (3, 6, and 8) are compared with the wild-type control. A, Phenotypes. B, Levels of RIN-MC protein. C, Accumulation of specific transcripts in transgenic tomato (AC *35S::FM-RIN-MC*) fruits at B+10. The western blots of fruits extracts from wild-type (AC) and RIN-MC-overexpressing plants in B used anti-myc antibody (top) with actin (bottom) as a control. In C, relative transcript levels were determined by RT-qPCR, relative to the expression of the tomato internal control *ACTIN* gene, expressed as $2^{-\Delta\Delta Ct}$ (Livak and Schmittgen, 2001). Lowercase letters indicate values with significant differences. At least three biological replicates were included for each assay.

efficient method to down-regulate the high expression of *RIN-MC* fusion genes in *rin* mutant fruit, in order to address this question. Two fragments specific to different regions of the *RIN-MC* fusion gene were selected for VIGS plasmid vector construction and used to generate pTRV2-*RIN* and pTRV2-*MC* (Supplemental Fig. S1, B and C). The pTRV2-*RIN* construct was used to silence the *RIN* gene in the wild type (AC) as the positive control (Supplemental Fig. S1A). Approximately 10 d after infiltration of the fruit stalk with mixed *Agrobacterium tumefaciens* strain GV3101 containing pTRV1 and pTRV2 constructs, fruits of the infiltrated plants developed an uneven coloring, and the *RIN*-silenced wild-type fruit (AC; positive control) displayed a partial yellow coloring phenotype symptomatic of ripening inhibition (Ito et al., 2015). Interestingly, silencing of *RIN-MC* genes, whether with pTRV2-*RIN* or pTRV2-*MC* vector, resulted in significantly patchy coloring of the fruits, with areas exhibiting different sections of yellow or green (Fig. 4A). The mRNA levels of the *RIN-MC* fusion gene in the yellow colored areas were reduced by more than 70% (Fig. 4B) compared with those in the green sectors, and the presence of the virus in the yellow areas was confirmed (Supplemental Fig. S1), indicating that silencing of *RIN-MC* accelerated the rate of ripening of *rin* fruit from green to yellow.

Global differences in ripening-related gene changes in the yellow parts of the *RIN-MC*-silenced *rin* fruit compared with the nonsilenced parts were explored by RNA sequencing, and 1,321 differentially expressed genes (DEGs) using the threshold of fragments per kilobase of exon model per million fragments mapped (FPKM) > 10, $\log_2$ fold change > 1, and $q < 0.01$ (Supplemental Data Set S1) were identified. Many DEGs known to be involved in the ripening process were influenced significantly by silencing the expression of the *RIN-MC* fusion gene, including some involved in cell wall metabolism and ethylene and carotenoid biosynthesis (Supplemental Fig. S2). The expression of a *Laccase1a* (Solyc10g085090) gene, which encodes a laccase involved in flavonoid and anthocyanin metabolism (DellaPenna et al., 1989), also was up-regulated in *RIN-MC*-silenced *rin* fruit and showed the largest fold change among all of the DEGs (up to 126-fold; Supplemental Data Set S1). Genes such as *GGPPS*, *LCYB1*, and *PSY1* in the MEP-carotenoid pathway (Enfissi et al., 2017) also were affected by *RIN-MC* silencing, suggesting that RIN-MC played a role in the regulation of carotenoid biosynthesis. The expression of *LoxC*, a lipoxygenase gene involved in flavor and volatile formation (Chen et al., 2004; Karlova et al., 2011), also was up-regulated in *RIN-MC*-silenced regions of *rin* fruit. In addition, some genes encoding fruit-specific transcriptional factors such as *NOR* and *HB-1* were influenced by *RIN-MC* silencing, as were several genes participating in the ethylene biosynthesis and signaling pathway, such as *SAM3*, *ETR6*, and *EIN3*

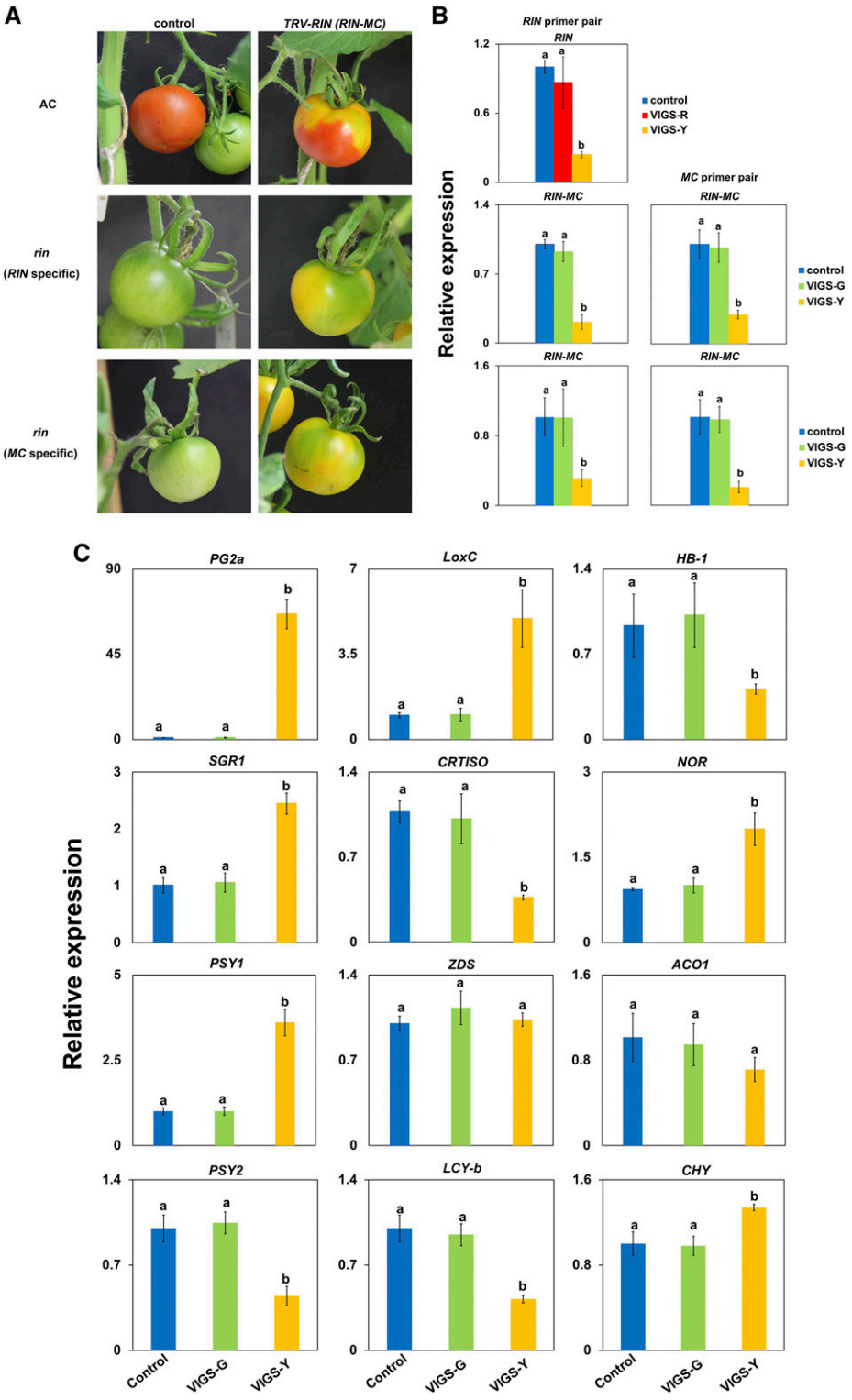

Figure 4. Effects of silencing *RIN* and *RIN-MC* on gene expression and affected ripening in wild-type (AC) and *rin* fruit. A, Phenotypes of silencing *RIN* and *RIN-MC* in wild-type and *rin* fruit (A). B and C, Gene expression assay of silenced *RIN* and *RIN-MC* genes (B) and ripening-related genes (C) analyzed using TRV-mediated VIGS in tomato fruits. The fruit stalks were injected with *A. tumefaciens* transformed with TRV alone or with pTRV2 carrying a fragment of the target gene (*RIN* in AC and *RIN-MC* in the *rin* mutant). Silencing *RIN* in wild-type (AC) fruit led to patchy red and yellowing, and silencing *RIN-MC* in the *rin* mutant led to uneven green and yellow coloring (A). RNA was extracted from the control and the different coloring areas of the gene-silenced tomato fruits. After reverse transcription, relative transcript levels were determined by RT-qPCR in the two parts of the fruits. Silencing of target genes led to significant decreases in gene expression (B). VIGS-R and VIGS-Y indicate the red and yellow parts of *RIN*-silenced fruits in the wild type, and VIGS-G and VIGS-Y indicate the green and yellow parts of *RIN-MC*-silenced fruits in the *rin* mutant (B and C). Relative transcript levels of some ripening-related genes were analyzed in *RIN-MC*-silenced fruits in the *rin* mutant (C).

(Supplemental Fig. S2). Changes in the expression of several important ripening genes identified by transcriptome analysis were studied by RT-qPCR assay (Fig. 4C). The results confirmed that silencing the expression of the *RIN-MC* fusion gene up-regulated the expression of *SGR1*, *LoxC*, *PG2a*, *NOR*, and *PSY1*, direct target genes of RIN, and the indirect target gene *CHY*, which showed coordinated regulation during tomato fruit ripening (Fujisawa et al., 2013; Zhong et al., 2013; Sakuraba et al., 2015). Silencing of *RIN-MC* also led to the inhibition of expression of *HB-1*, an HD-zip transcription factor; *CRTISO*, which encodes an enzyme involved in

carotenoid biosynthesis; *PSY2*, which is required for carotenoid biosynthesis; and *LCY-b*, involved in the MEP-carotenoid pathway (Enfissi et al., 2017). No significant changes were found in the expression of *CNR*, *ACO1*, *ETR4*, and *ZDS* in RT-qPCR analysis, however, which was consistent with the transcriptome analysis (Supplemental Fig. S2; Supplemental Data Set S1). These results indicated that the silencing of *RIN-MC* affected genes in various ripening-related pathways, implying a potential direct regulatory role of *RIN-MC* in tomato fruit ripening.

Difference in Phenotype between *RIN-MC*-Silenced and *rin* Fruit

The role of the *RIN-MC* fusion in the *rin* mutant was tested directly by expressing a *35S-RIN-MC* RNAi construct in transgenic *rin* fruit (*rin 35S::RIN-MC* RNAi plants). This led to a more rapid fruit color change to yellow, compared with the *rin* control (Fig. 5A; Supplemental Fig. S3C), and the yellow segments began to turn orange, with slight red color appearing at the BK+10 stage (Fig. 5A; Supplemental Fig. S3D). These results were very similar to those obtained by VIGS of *RIN-MC* (Fig. 4) and also were similar to the phenotype of AC::CRISPR-Cas9-*RIN* tomato fruit in a recent study (Ito et al., 2015). In our experiments, the fruit colors of AC *35S::RIN* RNAi and *rin* plants were easily distinguishable from BK+3 to BK+10 stages, with the most obvious difference being the late generation of an orange coloration in *RIN-MC* RNAi plants (Fig. 5; Supplemental Fig. S3).

The tomato fruit pericarp colors were measured with a colorimeter using the CIE L*a*b color system (Komatsu et al., 2016). The a* value refers to the degree of red to green, determined by the degradation of chlorophyll and the accumulation of carotenoids, such as β-carotene and lycopene, producing the characteristic yellow and red coloration (Luo et al., 2013). Wild-type (AC) fruits turned red gradually, but significantly different phenotypes were manifested by the three other kinds of fruits, with transgenic AC *35S::RIN* RNAi appearing orange-red and the *rin* mutant remaining yellow (Fig. 5; Supplemental Figs. S3 and S5A).

The color differences were confirmed by determining the concentrations of individual constituents of the carotenoid pathway in wild-type AC, AC *35S::RIN* RNAi, *rin*, and *rin 35S::RIN-MC* RNAi fruits at BK and BK+5 stages. Wild-type (AC) accumulated obvious lycopene at BK+5, and a small amount of lycopene was detected in tomato fruits of transgenic *rin 35S::RIN-MC* RNAi, while very little was detected in fruits of transgenic AC *35S::RIN* RNAi, and almost no lycopene was detected *rin* mutant fruits (Fig. 5C).

Differences in the expression of carotenoid biosynthesis genes were measured by RNA sequencing and

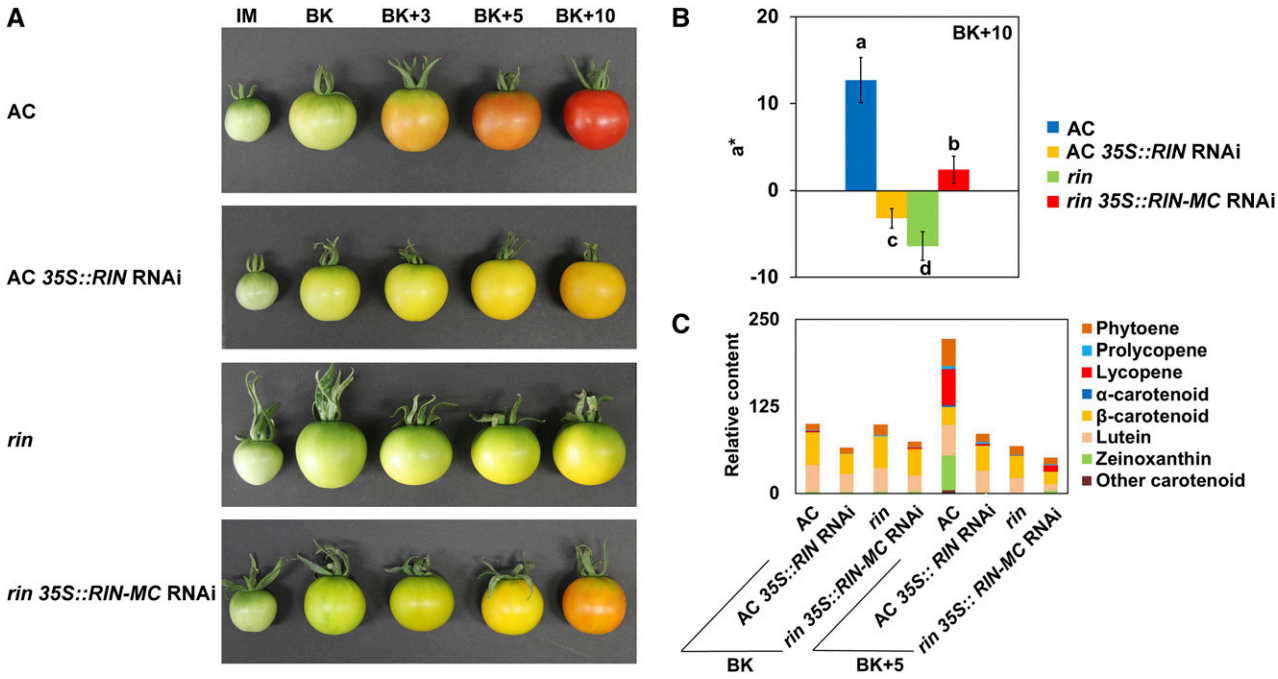

Figure 5. Effects of *RIN* and *RIN-MC* on fruit color and the accumulation of carotenoids. A, Phenotypes of four different lines: the wild type (AC), the wild type expressing a *RIN*-silencing construct, the *rin* mutant, and the *rin* mutant expressing a *RIN-MC*-silencing construct. B and C, Color (a*; B) and relative contents of carotenoids (C). For A, fruits were picked at IM, BK, BK+3, BK+5, and BK+10 stages. A hand-held colorimeter with the CIE L*a*b color system was used for pericarp color assay, and a* represents red to green (Komatsu et al., 2016). At least nine replicates were included for each assay. The contents of different carotenoids in each type of fruit are shown in C. At least three biological replicates were included for each assay.

visualized using the MapMan database (Usadel et al., 2009; Jaiswal and Usadel, 2016; Supplemental Fig. S4B). *RIN* RNAi inhibited the expression of all carotenoid biosynthesis genes tested, apart from *PSY2*, which is involved in carotenoid production in green fruit, prior to ripening (Fray and Grierson, 1993), and the greatest differences were found for *PSY1*, *ZDS*, *CrtISO*, *LCY-b*, and *CHY*. Key differences were found by comparing mRNAs in *rin* and *RIN* RNAi fruit, and these were confirmed by RT-qPCR (Supplemental Fig. S4C), which showed differences in transcripts of *LYC-b* and *CHY*. Furthermore, *RIN* RNAi failed to down-regulate *PSY2* compared with AC fruit, whereas this was reduced in *RIN-MC* RNAi fruit compared with *rin* fruit. Although small compared with *RIN-MC* RNAi fruit, there were significantly higher levels of *PSY1* mRNA, which is required for lycopene accumulation during ripening (Fray and Grierson, 1993).

Two other aspects of ripening, pericarp firmness and ethylene production, also were investigated in the wild type (AC), AC *35S*::*RIN* RNAi, *rin*, and *rin 35S*::*RIN-MC* RNAi at different stages of ripening. Only wild-type fruits showed a burst of ethylene synthesis and underwent softening, and there were no obvious differences in the pericarp firmness or ethylene production between the fruits of the *rin* mutant and the transgenic *rin 35S*::*RIN-MC* RNAi plants (Supplemental Fig. S5, B and C). Silencing of *RIN* gene expression in wild-type fruit significantly reduced the transcripts of genes involved in ethylene biosynthesis, such as *ACO1*, *ACS2*, and *ACS4*, and ethylene receptors, such as *ETR3* (Supplemental Fig. S5D). However, silencing of the *RIN-MC* fusion gene up-regulated the expression of genes involved in ethylene perception and response, such as *ERF6*, *ETR3*, and *EBF1* (Supplemental Fig. S5D), indicating that the normal function of RIN is as an activator of ethylene synthesis and perception; the down-regulation of *RIN-MC* in the *rin* mutant, however, was unable to restore ethylene production.

Comprehensive Analysis of RIN-MC-Regulated Genes

Expression of the *RIN-MC* fusion gene significantly affected coloring (Fig. 5; Supplemental Fig. S4) and other physiological traits (Supplemental Fig. S5) in ripening tomato fruit, and transcriptome analysis by RNA sequencing was performed in order to identify *RIN-MC* functions, using the threshold for DEGs of $\log_2$ fold change ≥ 1, $q < 0.05$, and FPKM > 10 for either sample, which discarded many genes with very low expression. Significant difference existed in comparison of wild-type (AC) with AC *35S*::*RIN* RNAi (AC/AC *35S*::*RIN* RNAi), comparison of *rin* mutant with *rin 35S*::*RIN-MC* RNAi (*rin*/*rin 35S*::*RIN-MC* RNAi), and comparison of AC with *rin* (AC/*rin*; Supplemental Fig. S6). Analysis of *rin*/*rin 35S*::*RIN-MC* RNAi identified 1,168 positively and 1,234 negatively DEGs (summarized in Fig. 6B; Supplemental Data Set S3). Most DEGs regulated by RIN-MC showed low identity ($r = 0.15$, $P =$ 7.72e-21; Fig. 6A) compared with those regulated by RIN (AC/AC *35S*::*RIN* RNAi; Fig. 6A), and genes in each subset in the Venn diagram (Fig. 6B) also are listed in Supplemental Data Sets S4 to S11.

Genes regulated by RIN-MC participate in various aspects of ripening, including Ethylene Receptor3 (*ETR3/NR*); cell wall metabolism, such as *PG2a*, polygalacturonase (*PGcat*), Pectinesterase1 (*PME1.9*), and *PME2.1*; carotenoid formation, such as *PSY1*, *PSY2*, and

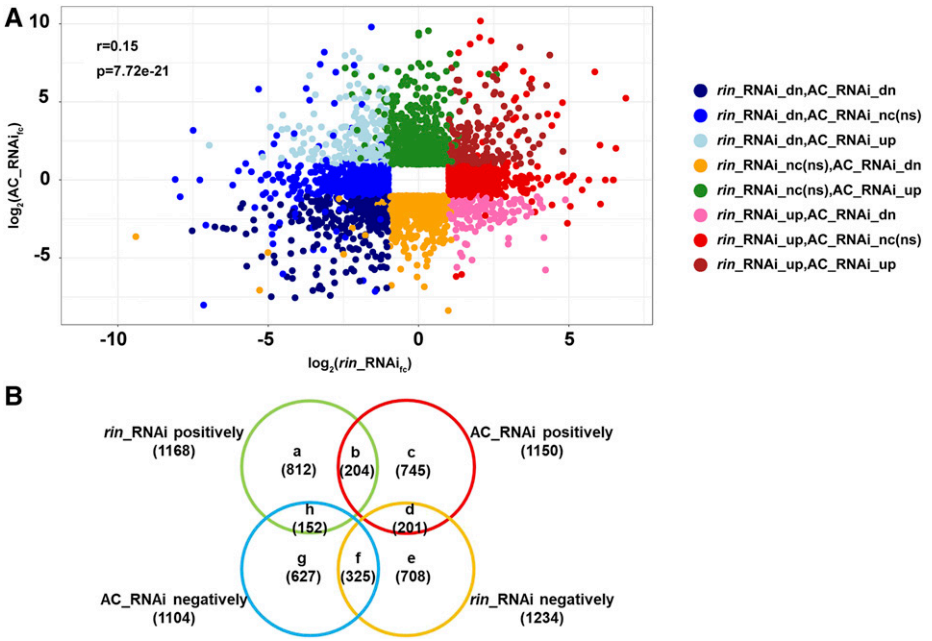

Figure 6. Comparison between DEGs in AC/AC *35S*::*RIN* RNAi and *rin*/*rin 35S*::*RIN-MC* RNAi. Scatterplot (A) and Venn diagram (B) of DEGs show comparisons between AC/AC *35S*::*RIN* RNAi and *rin*/*rin 35S*::*RIN-MC* RNAi. AC_RNAi, AC/AC *35S*::*RIN* RNAi; *rin*_RNAi, *rin*/*rin 35S*::*RIN-MC* RNAi; dn, down-regulated; fc, fold change; nc, no change; ns, no significant difference; up, up-regulated. Letters a to h are different regions in the Venn diagram. DEGs were selected with a threshold of $\log_2$ fold change ≥ 1, $q < 0.05$, and FPKM > 10 in each sample. RNA sequencing and DEG assay were for four genotypes of tomato fruits at the BK+5 stage, as mentioned in Supplemental Figure S4A and Figure 5. Genes in different regions in the Venn diagram are listed in Supplemental Data Sets S4 to S11.

geranylgeranyl pyrophosphate synthase (*GGPPS2*); and transcription factors, such as *TDR4* (Tables I and III; Supplemental Data Set S3). DEGs were categorized by Gene Ontology (GO) enrichment, and in a comparison between *rin* mutant and transgenic *rin 35S::RIN-MC* RNAi (*rin*/*rin 35S::RIN-MC* RNAi) (Supplementary Data Set 12), negatively regulated DEGs were enriched in three categories and positively regulated DEGs were enriched in only one category (biological process; Supplemental Fig. S7A). Groups such as thylakoid, response to abiotic

Table I. *Comparison of RIN and RIN-MC regulation in the expression of ripening genes*

Ripening-related genes were regulated by both RIN and RIN-MC, with the fold change given for each gene in AC/AC 35S::*RIN* RNAi (AC_RNAi) and in *rin*/*rin 35S::RIN-MC* RNAi (*rin*_RNAi).

Function	Description	Identifier	Gene	Differentially Expressed		ChIP_seq[a]	ChIP_chip[b]
				AC_RNAi	*rin*_RNAi		
Transcriptional factors	AP2-EREBP	*Solyc03g044300*	*Solyc03g044300*	1.53	0.29	Yes	Yes
	AP2-EREBP	*Solyc09g075420*	*ERF2*	6.84	0.27	Yes	No
	GRAS	*Solyc06g036170*	*GRAS9*	1.79	0.57	Yes	Yes
	MYB	*Solyc06g076770*	*Solyc06g076770*	2.59	0.21	No	Yes
	MADS	*Solyc06g069430*	*TDR4*	3.39	4.80	Yes	No
	GRAS	*Solyc02g085600*	*Solyc02g085600*	0.28	0.45	Yes	Yes
	C2H2	*Solyc04g077980*	*Solyc04g077980*	2.31	3.40	Yes	No
	bZIP	*Solyc08g006110*	*Opaque 2*	0.19	0.37	No	No
	HSF	*Solyc12g007070*	*Solyc12g007070*	0.53	0.32	Yes	No
	MADS	*Solyc05g012020*	*RIN* (*RIN-MC*)	2.84	3.51	Yes	Yes
	NAC	*Solyc10g006880*	*NAC-NOR*	0.49	0.52	Yes	Yes
	Auxin-responsive protein	*Solyc06g053840*	*Solyc06g053840*	2.47	2.92	No	Yes
	Histone-Lys *N*-methyltransferase NSD3	*Solyc01g103250*	*Solyc01g103250*	0.12	1.83	Yes	No
Ethylene	Synthesis	*Solyc01g095080*	*ACS2*	2.51	0.48	Yes	Yes
	Synthesis	*Solyc07g026650*	*ACO5*	99.11	5.59	No	No
	Receptors	*Solyc09g075440*	*ETR3/NR*	2.16	0.43	Yes	No
	Receptors	*Solyc09g089610*	*ETR6*	3.90	0.25	No	No
	Response	*Solyc01g009170*	*EIN3*	0.19	0.51	Yes	No
	Response	*Solyc12g009560*	*EBF1*	1.85	0.28	Yes	No
MEP-carotenoid pathway	Phytoene synthases	*Solyc03g031860*	*PSY1*	6.87	0.32	Yes	No
	9,15,9′-tri-cis-ζ-Carotene isomerase	*Solyc12g098710*	*ZISO*	2.65	0.19	Yes	Yes
	Nonheme hydroxylases	*Solyc03g007960*	*CHY*	2.47	0.17	Yes	No
	Geranylgeranyl pyrophosphate synthases	*Solyc04g079960*	*GGPPS2*	0.66	0.25	No	No
	Lycopene β-cyclases	*Solyc04g040190*	*LCY-b*	2.18	3.33	No	Yes
Flavonoid/ anthocyanin	4-Coumarate-CoA ligase	*Solyc03g117870*	*4CL*	1.96	0.38	Yes	Yes
	Phe ammonia lyase	*Solyc05g056170*	*PAL*	0.18	0.48	Yes	No
Cell wall	Endo-1,4-β-glucanase	*Solyc01g102580*	*Cel3*	1.83	0.30	Yes	Yes
	Endo-1,4-β-glucanase	*Solyc05g005080*	*Cel6*	0.45	2.28	No	No
	Expansin-like protein precursor (EXLA1)	*Solyc01g112000*	*LeEXLA1*	3.93	0.10	Yes	No
	LeXYL1	*Solyc10g047030*	*LeXYL1*	3.11	0.23	Yes	No
	Xyloglucan endotransglucosylase hydrolase XTH3	*Solyc03g093120*	*SlXTH3*	4.04	0.10	No	No
	Extensin (class II)	*Solyc11g005150*	*tegII*	2.80	0.03	Yes	No
	Arabinosidase ARA-1	*Solyc10g081120*	*ARA-1*	0.20	1.64	No	No
	Expansin precursor (EXPA5)	*Solyc02g088100*	*EXPA5*	0.16	0.48	No	No
	Fruit ripening-regulated expansin	*Solyc06g051800*	*LeEXP1*	8.39	10.13	Yes	Yes
	β-Fructofuranosidase, cell wall invertase	*Solyc09g010080*	*lin5*	0.18	0.14	No	No
	Dehiscence polygalacturonase	*Solyc04g015530*	*PS-2*	0.01	0.38	No	No
	Arabinogalactan	*Solyc02g092790*	*AGP-1c*	0.52	0.05	Yes	Yes
	Expansin (EXPA6)	*Solyc10g086520*	*EXPA6*	0.34	0.04	Yes	No
	Polygalacturonase	*Solyc08g060970*	*PGcat*	7.51	6.49	No	No
	Pectinesterase2.1	*Solyc07g064180*	*PME2.1*	0.43	0.10	No	No
	Endoxyloglucan transferase	*Solyc04g008210*	*SlXTH8*	0.35	0.13	No	No
	β-Galactosidase precursor	*Solyc12g044880*	*TBG1*	2.03	2.19	No	No
	β-Galactosidase	*Solyc03g019890*	*TBG7*	9.89	3.18	No	No

[a]Chromatin immunoprecipitation sequencing data from Zhong et al. (2013). [b]ChIP-chip data from Fujisawa et al. (2012).

stimulus, and signal transduction were highly enriched (Supplemental Fig. S7A). Many DEGs involved in ripening were negatively regulated by RIN-MC, indicating that the *RIN-MC* fusion gene might play an inhibitory role, which was consistent with the results of both VIGS (Fig. 4) and its inhibition of red coloring (Fig. 5) in tomato fruit ripening. In contrast, DEGs positively regulated by RIN were associated with known ripening pathways (Supplementary Data Set 13), consistent with the widely recognized role of RIN as a ripening activator. DEGs regulated by RIN-MC were highly enriched in metabolic pathway and biosynthesis of secondary metabolites by Kyoto Encyclopedia of Genes and Genomes (KEGG) pathway enrichment analyses, and DEGs regulated by RIN were highly enriched in biosynthesis of secondary metabolites (Supplemental Fig. S7B; Supplementary Data Set 14 and 15). These results indicate significant regulatory differences between RIN-MC and MADS-RIN, although their MADS-box domains are homologous.

RIN-MC Protein Has Transcription Factor Activity

The predicted domain structures of the RIN-MC protein (Fig. 2A) are likely to be sufficiently similar to the regular structure of MADS transcription factors to be able to participate in target promoter binding and possibly protein dimerization (Kaufmann et al., 2005). Accordingly, the subcellular localization and trans-activation

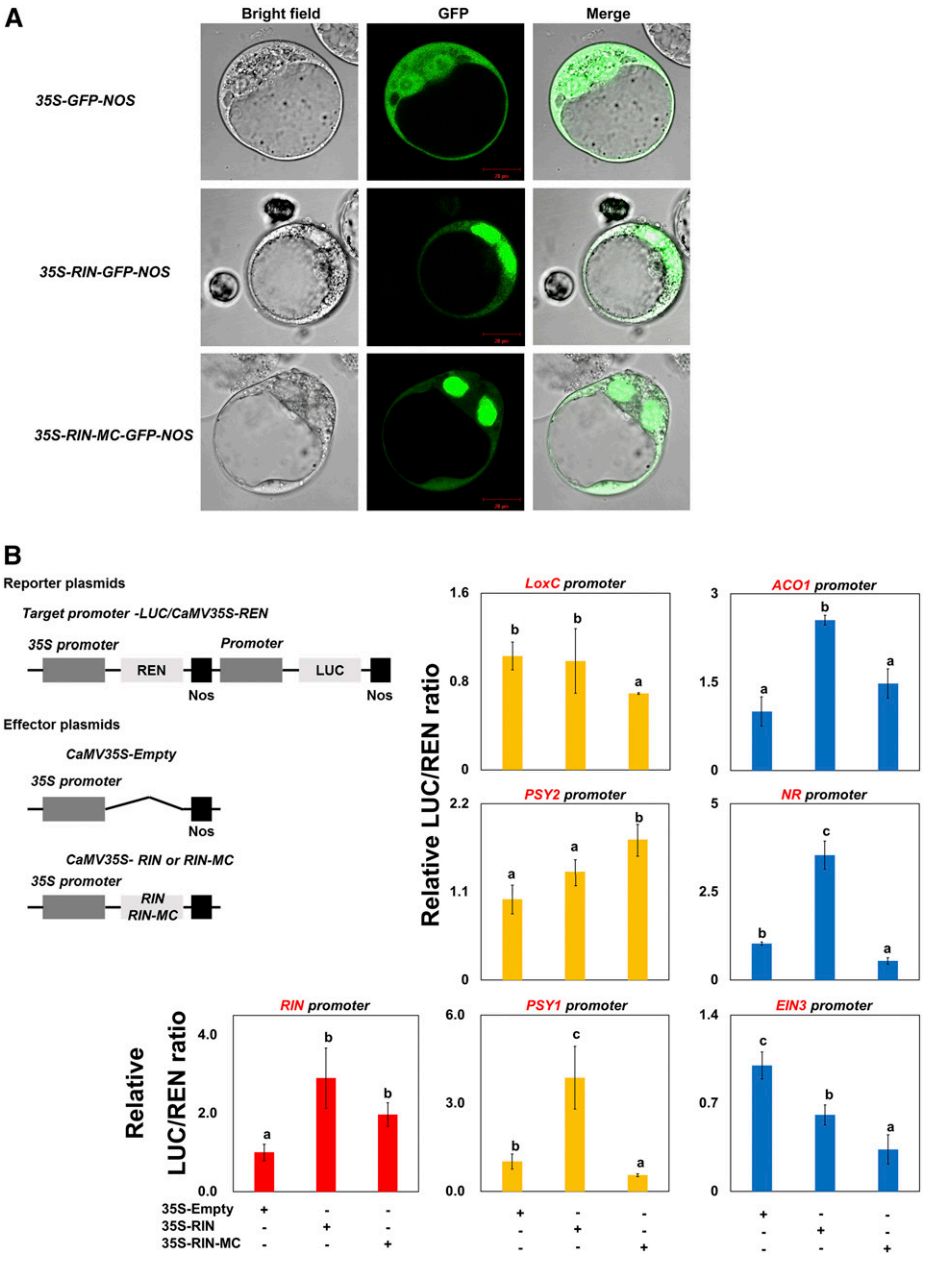

Figure 7. Transcription factor activity of RIN-MC protein. Subcellular localization (A) and trans-activation assay (B) of RIN-MC for RIN-MC protein are shown. In the subcellular localization assay (A), BY2 cell protoplasts were transiently transformed with RIN-GFP or RIN-MC-GFP constructs or GFP vector using the polyethylene glycol method. GFP fluorescence was observed with a fluorescence microscope. Trans-activation activities of tomato RIN and RIN-MC (B) were analyzed in the *N. benthamiana* transient expression system, using the double-reporter plasmid containing the promoters of ripening genes fused to LUC luciferase and REN luciferase driven by CaMV 35S. The effectors were RIN or RIN-MC driven by CaMV 35S. The effector and reporter plasmids were transfected into *A. tumefaciens* separately and coinfected into *N. benthamiana* leaves. The luciferase was measured 2 to 5 d after infiltration. At least nine biological replicates were included for each assay. The lowercase indicates significant difference.

activities of RIN-MC protein were analyzed in vivo, and RIN-MC fused to GFP protein was shown to be localized in nuclei, as found for RIN (Fig. 7A).

The trans-activation capability of the RIN-MC chimeric protein was tested by transient dual luciferase (LUC) reporter assays in *N. benthamiana* leaves. Promoters of potential target genes were fused to the LUC reporter separately, with a Renilla (REN) reporter under the control of the 35S promoter as an internal control, and tested against either the RIN or RIN-MC protein. The RIN-MC protein activated the *LUC* reporter gene when driven by *RIN* promoter segments of 2, 1.5, 1, and 0.75 kb compared with the empty vector negative control (Supplemental Fig. S8), but there was no activity with a 0.5-kb *RIN* promoter fragment, as also found for the RIN protein, indicating a requirement for sufficient length of promoter to contain important regulatory motifs (Fujisawa et al., 2013). RIN-MC activated the expression of *PSY2*, which is required for carotenoid biosynthesis; genes such as *LoxC*, *PSY1*, *NR*, and *EIN3* were repressed by RIN-MC, whereas it had no significant trans-activation on the *ACO1* promoter (Fig. 7B). These responses were different from those observed with RIN, particularly for target genes such as *LoxC*, *ACO1*, *PSY2*, *NR* (*ETR3*), and *PSY1*. Both RIN-MC and RIN, on the other hand, inhibited expression from the *EIN3* promoter (Fig. 7B).

MADS-box transcription factors usually form protein complexes in vivo, and the predicted RIN-MC protein contains the complete MADS-box domain from RIN, which could interact physically with other important ripening regulators such as FUL1 and FUL2 (Shima et al., 2013; Fujisawa et al., 2014), MADS1 (Dong et al., 2013), and TAGL1 (Itkin et al., 2009; Fujisawa et al., 2014). Accordingly, these four MADS-box factors were selected as potential targets to analyze protein-protein interactions with the RIN-MC fusion protein. Initially, the interactions between RIN-MC and FUL1, FUL2, MADS1, and TAGL1 were performed by colocalization assays using bimolecular fluorescence complementation (BiFC) technology. The *RIN* and *RIN-MC* genes were constructed with an N-terminal YFP coding sequence to generate a chimeric protein, and the four MADS-box genes were constructed with C-terminal YFP sequences. RIN-MC interacted with FUL1, FUL2, MADS1, and TAGL1 (Fig. 8), and the BiFC assays also showed that RIN colocalized and interacted with these MADS-box factors in cell nuclei. These results were very similar to those demonstrated for RIN in previous studies (Martel et al., 2011; Dong et al., 2013; Shima et al., 2013; Fujisawa et al., 2014).

To confirm the interaction between RIN-MC and FUL1, FUL2, MADS1, and TAGL1 observed in the BiFC

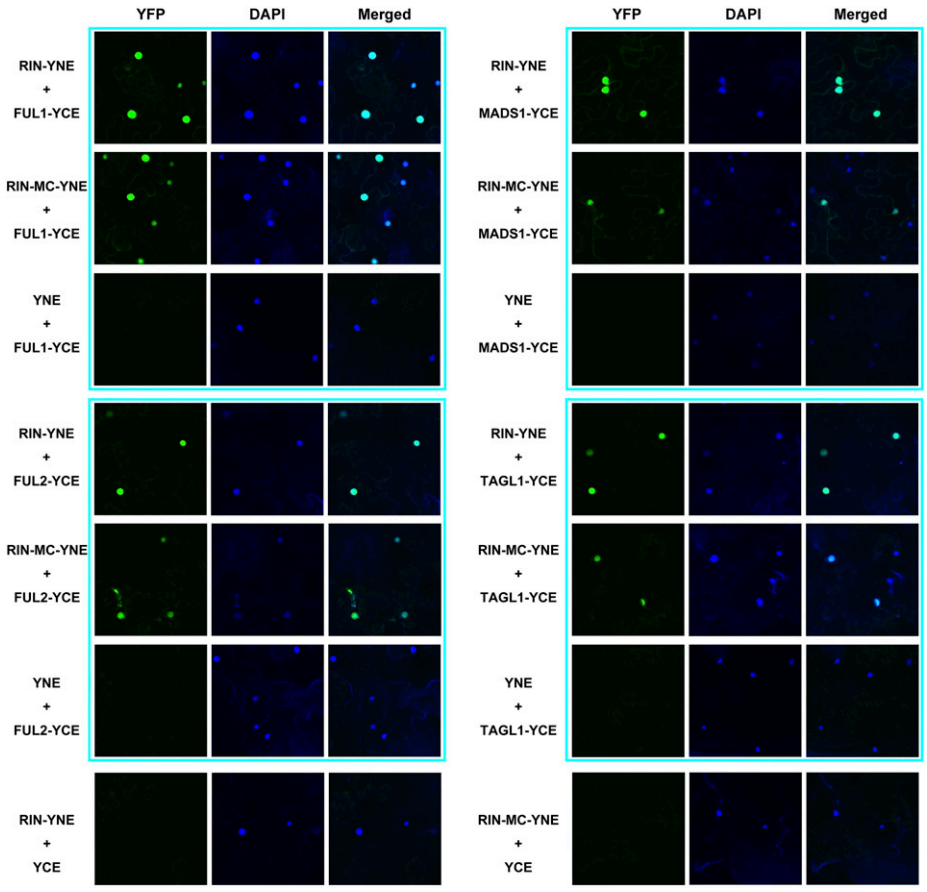

Figure 8. Interactions between RIN and RIN-MC with MADS-box factors measured by BiFC assay. RIN or RIN-MC was fused with the N-terminal end of YFP (YNE), and FUL1, FUL2, TAGL1, and MADS1 were fused individually with the C-terminal end of YFP (YCE). The expression of RIN/RIN-MC or FUL1/FUL2/TAGL1/MADS1 alone was used as a negative control. 4′,6-Diamino-phenylindole (DAPI) staining was included as a control for nuclear localization.

assay, coimmunoprecipitation (CoIP) assays were performed. Full-length RIN or RIN-MC (with a deleted stop codon) plus a C-terminal 6myc tag (RIN-6myc and RIN-MC-6myc) and MADS-box factors (FUL1-3HA, FUL6HA, MADS1-3HA, and TAGL1-3HA) with C-terminal 3HA tags were coexpressed in *N. benthamiana* leaves. The results showed that FUL1-3HA, FUL2-3HA, MADS1-3HA, and TAGL1-3HA coimmunoprecipitated with RIN-MC-6myc (Fig. 9A). Similar results also were observed when these MADS-box factors with 3HA tags also were coimmunoprecipitated with RIN-6myc (Fig. 9B).

DISCUSSION

In this study, we investigated the possible functions of the *RIN-MC* fusion gene in fruit of the *rin* tomato mutant. Our results showed that the RIN-MC fusion protein accumulated to a high level in *rin* fruit. Overexpression of RIN-MC in wild-type fruit impaired several ripening changes, and silencing of *RIN-MC* expression led to these fruit turning weakly red. GFP localization, BiFC, and CoIP assays suggested that RIN-MC could associate physically with FUL1, FUL2, MADS2, and TAGL1 and form potential heteroprotein complexes in planta, and trans-activation studies indicated that RIN-MC had transcription factor activity.

Gene Fusions Can Play an Important Role in Developmental Biology

Important biological effects of gene fusion can result from chromosomal rearrangements, DNA shuffling, abnormal transcription, and alternative splicing, leading to the formation of chimeric proteins that can have significance in human cancer (Mitelman et al., 2007; Annala et al., 2013). The altered chimeric protein can constitutively activate downstream target genes or destroy a critical cellular function (Annala et al., 2013), such as the chimeric BCR-ABL1 in leukemia (McWhirter et al., 1993), FGFR3-TACC3 fusions in glioblastoma (Singh et al., 2012), and the ALK fusions in anaplastic large cell lymphoma (Chiarle et al., 2008). The reports of gene fusion relevant to plant metabolism are limited, but at least two gene fusion events have been confirmed as relevant to benzylisoquinoline alkaloid metabolism (Li et al., 2016; Hagel and Facchini, 2017). This disparity probably reflects a knowledge gap concerning plant gene fusions rather than a reduced occurrence of functional importance compared with studies related to human disease. It also has been reported that a considerable number of fusion mRNAs might produce chimeric proteins in Arabidopsis and rice (Shahmuradov et al., 2010). Moreover, regardless of the specific mechanism involved in gene fusion, the final multidomain enzymes, particularly those sharing domain-level homology with different enzyme types, might function in metabolic pathways (Boycheva et al., 2014; Nützmann and Osbourn, 2014), as in the enormous diversity of terpene synthases found in plants (Zi et al., 2014).

However, in our experiments, we investigated the potential role of the fusion of adjacent transcription factor genes resulting from a genomic DNA fragment deletion (Vrebalov et al., 2002) and showed that the fusion protein was expressed abundantly in ripening fruit (Fig. 2), accumulated in the nucleus (Fig. 7), interacted with other transcription factors (Figs. 8 and 9), and altered the transcriptome and ripening phenotype (Fig. 6; Supplemental Fig. S3), which would help promote studies related to gene fusion in plants.

RIN-MC Transcripts and Protein Are Present in Abundance in *rin* Fruit

The RIN transcription factor is widely recognized as one of the hub regulators controlling ripening, and the *rin* mutation results in a severely ripening-inhibited phenotype (Vrebalov et al., 2002). At the transcriptional level, the expression of numerous genes involved in almost all branches of the ripening-related pathways is affected (Qin et al., 2012; Fujisawa et al., 2013, 2014). Our understanding of the role of RIN has been based on the characterization of *rin* mutant fruit, in which the fruit-specific factor RIN is impaired by the formation of the *RIN-MC* fusion, whereas the normal MC was believed not to be a fruit regulator (Vrebalov et al., 2002).

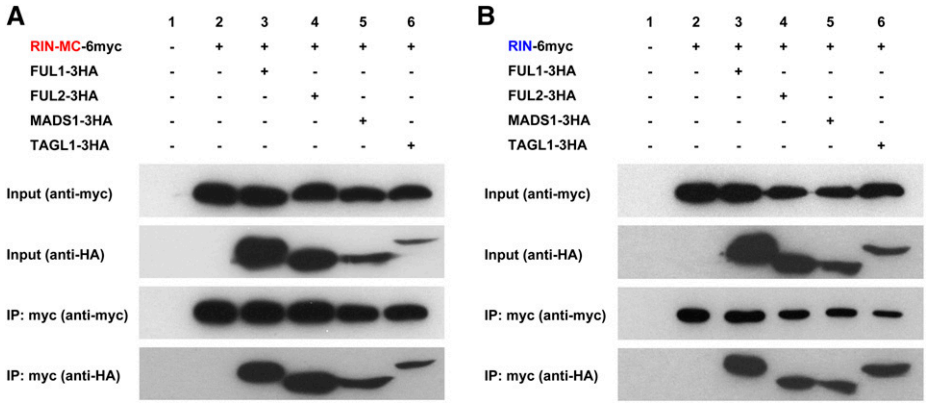

Figure 9. Interactions between RIN-MC and RIN and MADS-box factors measured by CoIP. Total protein extracts (Input) and protein complexes immunoprecipitated with anti-myc agarose (IP) were separated on gels and blotted. RIN-MC and MADS-box factors interacted (A), similar to RIN (B) interactions measured by CoIP. Anti-HA and anti-myc antibodies were used in western blotting.

In most previous studies, the expression of *RIN-MC* was found to be low (Vrebalov et al., 2002; Martel et al., 2011; Fujisawa et al., 2012, 2013), but recently, it was shown, based on RNA sequencing technology, that *rin* mutant fruit accumulate high levels of *RIN-MC* transcripts at 42 DPA and at the pink ripening stage (Zhong et al., 2013; Fujisawa et al., 2014). In previous studies, the specific *RIN-MC* fusion gene fragments detected mapped mainly to part of the 3′ region of the normal *RIN* gene, which is absent from the *rin* mutant, explaining why almost no transcript signals were detected. For example, probes used for northern blotting were homologous to the 3′ untranslated region of *RIN* (Vrebalov et al., 2002), probe sets selected for microarrays mapped mostly to the missing region of the *RIN* gene (Fujisawa et al., 2012), and primer pairs designed for RT-qPCR amplification were targeted to fragments that do not exist in their entirety in the *RIN-MC* fusion gene (Martel et al., 2011; Fujisawa et al., 2013). Recently, the high expression level of *RIN-MC* was determined from transcriptome data derived by high-throughput sequencing technology (Zhong et al., 2013; Fujisawa et al., 2014), and this was confirmed at both the RNA and protein levels in this study (Figs. 1 and 2). A polyclonal antibody against RIN partial protein also was used to detect RIN-MC protein successfully in the *rin* mutant in this study, unlike previous reports (Ito et al., 2008; Martel et al., 2011; Qin et al., 2012). The MC-specific antibody is much more suitable for distinguishing the RIN-MC fusion protein in *rin* fruit, because minor signals from translational products of the *MC* gene exist in ripening fruits of wild-type AC (Vrebalov et al., 2002).

The Role of RIN-MC in Gene Expression in *rin* Mutant Fruit

The RIN transcription factor is a central regulator in tomato fruit ripening (Vrebalov et al., 2002), and *RIN* is expressed in a fruit ripening-specific pattern, which has almost no abundance of transcripts in other tissues such as bud, leaf, root, and immature green (IG) fruits (Tomato Genome Consortium, 2012). As a result, the regulation of RIN and RIN-MC in tomato fruit ripening was much more focused. Genes regulated by RIN-MC participate in various aspects of ripening, including *ETR3/NR*; cell wall metabolism, such as *PG2a*, *PGcat*, *PME1.9*, and *PME2.1*; carotenoid formation, such as

Table II. *Comparison of RIN and RIN-MC regulation in the expression of ripening genes*

Ripening related genes regulated by RIN-MC but not RIN, with the fold change for each gene in *rin*/*rin 35S*::*RIN-MC* RNAi. AC_RNAi, AC/AC 35S::RIN RNAi; *rin*_RNAi, *rin*/*rin 35S*::*RIN-MC* RNAi; ChIP-seq data are from Zhong et al., 2013; the ChIP-chip data from Fujisawa et al., 2012.

Function	Description	Identifier	Gene	Differentially Expressed		ChIP_seq[a]	ChIP_chip[b]
				AC_RNAi	*rin*_RNAi		
Transcriptional factors	AP2-EREBP	*Solyc01g065980*	*ERF2b*	No	0.46	Yes	No
	AP2-EREBP	*Solyc03g093560*	*ERF5*	No	1.82	No	No
	AP2-EREBP	*Solyc03g093540*	*ERF1a*	No	3.55	No	No
	AP2-EREBP	*Solyc12g009240*	*ERF4*	No	7.83	No	No
	AP2-EREBP	*Solyc02g077370*	*Pti5*	No	3.19	No	No
	ARF	*Solyc02g037530*	*ARF8*	No	2.68	Yes	No
	bZIP	*Solyc01g079480*	*bZIP-1*	No	0.41	No	No
	bZIP	*Solyc04g011670*	*Solyc04g011670*	No	3.08	No	No
	C2C2-CO-like	*Solyc08g006530*	*Solyc08g006530*	No	6.53	No	No
	C2H2	*Solyc08g063040*	*Solyc08g063040*	No	0.31	Yes	Yes
	CCAAT	*Solyc01g006930*	*Solyc01g006930*	No	2.51	No	No
	GRAS	*Solyc07g052960*	*Solyc07g052960*	No	0.24	Yes	Yes
	HB	*Solyc05g006980*	*Solyc05g006980*	No	2.10	No	No
	HB	*Solyc02g063520*	*Solyc02g063520*	No	4.41	Yes	No
	LIM	*Solyc04g077780*	*Solyc04g077780*	No	3.87	No	No
	MYB	*Solyc03g113620*	*Solyc03g113620*	No	1.90	No	No
	WRKY	*Solyc09g014990*	*Solyc09g014990*	No	4.66	No	No
	GRAS	*Solyc11g013150*	*Solyc11g013150*	No	2.94	No	No
Transcriptional regulator	Auxin-responsive protein	*Solyc03g120500*	*Solyc03g120500*	No	1.93	Yes	Yes
MEP-carotenoid pathway	Phytoene synthases	*Solyc02g081330*	*PSY2*	No	2.99	Yes	No
	Zeaxanthin epoxidase	*Solyc02g090890*	*ZEP*	No	3.44	Yes	No
Flavonoid/ anthocyanin	4-Coumarate-CoA ligase	*Solyc11g069050*	*4CL*	No	2.92	Yes	No
	Lipoxygenase	*Solyc01g006540*	*LoxC*	No	0.20	Yes	Yes
Cell wall	Endo-1,4-β-mannanase	*Solyc01g008710*	*LeMAN4a*	No	0.03	Yes	No
	LeXYL2	*Solyc01g104950*	*LEXYL2*	No	0.26	Yes	No
	Polygalacturonase2a	*Solyc10g080210*	*PG2a*	No	0.01	Yes	No
	Pectinesterase1	*Solyc07g064170*	*PME1.9*	No	0.05	No	No
	β-Galactosidase	*Solyc12g008840*	*TBG4*	No	0.39	Yes	No
	S-Galactosidase	*Solyc03g121540*	*teg1A/TBG3*	No	2.81	Yes	No

[a]ChIP-seq data from Zhong et al. (2013). [b]ChIP-chip data from Fujisawa et al. (2012).

Table III. *Comparison of RIN and RIN-MC regulation in the expression of ripening genes*

Ripening-related genes were regulated by RIN but not RIN-MC, with the fold change for each gene in AC/AC 35S::*RIN* RNAi. AC_RNAi, AC/AC 35S::RIN RNAi; *rin*_RNAi, *rin*/*rin 35S*::*RIN-MC* RNAi.

Function	Description	Identifier	Gene	Differentially Expressed		ChIP_seq[a]	ChIP_chip[b]
				AC_RNAi	*rin*_RNAi		
Transcriptional factors	bZIP	*Solyc01g100460*	*abz1*	2.67	No	Yes	Yes
	C2C2-CO-like	*Solyc12g096500*	*Solyc12g096500*	0.16	No	Yes	Yes
	SBP	*Solyc02g077920*	*LeSPL-CNR*	1.66	No	Yes	Yes
	ULT	*Solyc07g054450*	*Solyc07g054450*	1.52	No	Yes	Yes
	WRKY	*Solyc02g021680*	*Solyc02g021680*	4.04	No	Yes	No
	GRAS	*Solyc01g008910*	*Solyc01g008910*	2.75	No	Yes	Yes
	GRAS	*Solyc11g012510*	*GRAS1*	0.27	No	Yes	No
Transcriptional regulator	Auxin-responsive protein	*Solyc03g120390*	*Solyc03g120390*	0.29	No	Yes	Yes
	Transcription elongation factor A protein2	*Solyc10g080930*	*Solyc10g080930*	2.19	No	No	No
	DNA-repair protein	*Solyc06g050510*	*Solyc06g050510*	0.54	No	No	No
Ethylene	Synthesis	*Solyc07g049550*	*ACO3*	16.02	No	Yes	No
	Synthesis	*Solyc05g050010*	*ACS4*	4.93	No	Yes	Yes
	Synthesis	*Solyc07g049530*	*ACO1*	4.70	No	Yes	No
	Receptors	*Solyc06g053710*	*ETR4*	2.54	No	Yes	No
	Response	*Solyc06g073730*	*EIL4*	2.22	No	No	No
	Response	*Solyc08g060810*	*EBF2*	0.50	No	Yes	Yes
	Response	*Solyc03g111720*	*E4*	3.39	No	No	No
MEP-carotenoid pathway	Isopentenyl diphosphate isomerases	*Solyc05g055760*	*IPP2*	0.22	No	No	No
	ζ-Carotene desaturase	*Solyc01g097810*	*ZDS*	2.57	No	No	No
	7,9,7′,9′-tetra-cis-Lycopene isomerase	*Solyc10g081650*	*CrtISO*	3.15	No	Yes	Yes
	Alternative oxidase	*Solyc11g011990*	*PTOX*	2.55	No	Yes	No
	P450 hydroxylases	*Solyc04g051190*	*CYP97A3*	0.44	No	No	No
Cell wall	Endo-1,4-β-glucanase	*Solyc09g010210*	*Cel2*	270.30	No	Yes	Yes

[a]ChIP-seq data from Zhong et al. (2013). [b]ChIP-chip data from Fujisawa et al. (2012).

PSY1, *PSY2*, and *GGPPS2*; and transcription factors, such as *TDR4* (Tables I and III; Supplemental Data Set S3). Moreover, nuclear localization and interaction studies with other transcription factors showed that RIN-MC protein had the expected characteristics of a transcription factor. Although RIN-MC protein could, like RIN, form MADS-box complexes with FUL1, FUL2, MADS1, and TAGL1 (Figs. 8 and 9), the regulatory effects on target genes were not so similar to those found for RIN (Tables I and III; Supplemental Data Set S2). For genes such as *TDR4* and *LCY-b*, *RIN-MC* silencing reduced their expression, similar to the effect induced by *RIN* silencing (Table I). The comparison of AC/AC *35S*::*RIN* RNAi and *rin*/*rin 35S*::*RIN-MC* RNAi, however, (Table I), showed opposite trends for genes such as *ERF2*, *GRAS9*, *ACS2*, *NR*, *EBF1*, *PSY1*, *ZISO*, *4CL*, and *Cel3*. More interestingly, the expression of genes such as *ERF2b*, *ARF8*, *LoxC*, *LeMAN4a*, *PG2a*, and *TBG4* was not affected by *RIN* silencing; these genes were expressed significantly in comparison with *rin*/*rin 35S*::*RIN-MC* RNAi (Table II).

Genes regulated by RIN-MC participated not only in fruit-ripening processes but also in many other aspects, such as ascorbate biosynthesis and recycling, cell wall structure, resistance to stress, protein modification, and some kinase, which indicated that RIN-MC regulation spreads in various important biological aspects (for details, see Supplemental Data Sets S2 and S3). The amounts of genes regulated by RIN-MC had different regulation patterns by RIN in ascorbate biosynthesis and recycling. Genes such as dehydroascorbate reductase and GDP-L-Gal phosphorylase (*GGP2*), which were key regulators of fruit ascorbic acid concentrations (Mellidou et al., 2012), were significantly regulated by RIN-MC but not RIN. The cytochrome P450 monooxygenase (P450) superfamily is involved in the biosynthesis of various primary and secondary metabolites (Yu et al., 2017). Genes encoding cytochrome P450, such as *CYP71D208* and *CYP90B3*, were obviously up-regulated by RIN-MC but could not be induced by RIN. Genes regulated by RIN-MC but not by RIN also were involved in resistance to stress and ubiquitination, such as multi-antimicrobial extrusion protein (Solyc05g013460), hairpin-induced protein (*Solyc03g121620*), ubiquitin-like (*Solyc05g056060*), and ubiquitin-conjugating enzyme (*Solyc10g012240*). Meanwhile, many DEGs showed different regulation patterns by RIN and RIN-MC, such as glycoside hydrolase (*Solyc01g067660*), UDP-glucosyltransferase (*Solyc02g070020*), lipoxygenase (*Solyc01g006540*), and lipase (*Solyc03g005020*), involved in carbohydrate and lipid metabolism. All these genes were targets of RIN, except *GGP2* and *CYP71D208*. Comparison between RIN and RIN-MC regulation in fruit ripening and other processes offered valuable clues for further identification of new functions of RIN-MC in future studies.

Furthermore, differences in trans-activating activities were distinguished between RIN and RIN-MC. Taking the results for *LoxC* and *PSY2* as examples, RIN had no significant trans-activating activity, but RIN-MC regulated their expression (Fig. 7), which indicated that RIN-MC has its own independent transcriptional activity in planta. For RIN target genes, such as *CNR*, *ACO3*, and *ACS4*, expression was influenced by *RIN* silencing but not by *RIN-MC* silencing, which also indicates different mechanisms of action of RIN-MC protein and RIN on the same target genes (Table III). Meanwhile, RIN-MC could activate the *LUC* reporter gene when driven by the *RIN* promoter (Fig. 7; Supplemental Fig. S8), which is consistent with the up-regulation of *RIN-MC* expression in tomato fruit (Fig. 1B), indicating a similar positive regulatory feedback to RIN. These findings are in disagreement with the conclusion from a previous study, in which the *RIN-MC* fusion gene expressed in yeast cells was transcriptionally inactive (Ito et al., 2008). This discrepancy may be related to differences in transcriptional activation by RIN-MC protein in tobacco (*Nicotiana tabacum*) leaves and yeast cells, differences in regulating target genes, or the effects of differences in the ability to form protein complexes between the RIN-MC protein and other proteins recruited in vivo in yeast and tobacco. Bioinformatics analysis showed that an ERF-associated amphiphilic repression motif (LDLNL; Ohta et al., 2001) is present in the C terminus of the RIN-MC protein (Supplemental Fig. S9), which might explain the repression effect of RIN-MC on some target genes (Fig. 7). These results show that the RIN-MC fusion protein has a separate and distinct function from the normal and mutated RIN. Silencing *RIN-MC* in the *rin* mutant (*rin 35S::RIN-MC* RNAi fruits), where the mRNA was reduced to 4.2% (Supplemental Fig. S4A), could not restore the normal ripening process and only resulted in weak red coloration without an ethylene burst (Fig. 5; Supplemental Figs. S3–S5). Overexpressing the RIN protein in *rin*::CRISPR/Cas9-*RIN-MC* fruit would be expected to restore normal fruit ripening.

In conclusion, the possibility that RIN-MC plays a role in controlling the expression of ripening genes in the *rin* mutant has not received much credence previously because the evidence indicated that its transcripts were absent from the mutant fruit (Martel et al., 2011; Fujisawa et al., 2012, 2013). We have shown that *rin* fruit in fact contain abundant *RIN-MC* mRNA, which is translated. The encoded protein is located in the nucleus, interacts with other MADS-box transcription factors, and is capable of altering ripening gene expression when overexpressed in wild-type fruit. Further work will be necessary to identify all the gene targets of RIN-MC and to determine the transcriptional interactions between RIN-MC, other transcription factors, and target gene promoters.

MATERIALS AND METHODS

Plant Material and Growth Conditions

Wild-type tomato (*Solanum lycopersicum* AC) and *rin* mutant (AC background) seedlings were grown in a greenhouse under long-day conditions (16 h of light and 8 h of dark) at a temperature of 26°C. For gene expression analysis, organs were collected, frozen in liquid nitrogen, and stored at −80°C until RNA extraction. Three independent samplings were performed.

Primers

All the primers designed and used in this study are listed in Supplemental Tables S1 and S2.

Tomato Genetic Transformation

The recombined pCAMBIA1300-*35S-FM-RIN-MC* vector was selected for protein overexpression in transformed tomato. A hairpin-inducing vector harboring two gene-specific fragments (targeting either *RIN* or *RIN-MC*) was chosen for gene silencing based on an RNAi strategy. The *Agrobacterium tumefaciens*-mediated transfer of T-DNA was used for stable transformation of tomato (Sun et al., 2006; Kimura and Sinha, 2008). At least three lines were obtained for each assay.

RNA Isolation and RT-qPCR

RNA was isolated from pericarp of tomato fruits at different ripening stages as described (Zhu et al., 2015). Total RNA extraction from tomato fruit pericarp was carried out using DeTRNa reagent (EarthOx) according to the manufacturer's protocol, and RNA integrity was verified by 1.5% (v/v) agar gel electrophoresis. Genomic DNA was removed from RNA preparations by digestion with DNase I (TaKaRa), and RNA quality and quantity were confirmed by spectrophotometry (Thermo Scientific; NanoDrop 1000). RNA was reverse transcribed into cDNA using M-MLV Reverse Transcriptase (Promega) according to the manufacturer's instructions. RT-qPCR was conducted using TransStart Top Green qPCR SuperMix (Transgen) with the CFX96 Real-Time PCR System (Bio-Rad). Relative gene expression values were calculated using the $2^{-\Delta\Delta Ct}$ method (Livak and Schmittgen, 2001). The tomato *ACTIN* gene (Solyc03g078400) was used as an internal reference gene. At least three biological replicates were included for each point, and each replicate was from independent sampling.

Ethylene and 1-MCP Treatment

Tomato fruits at the MG stage were placed into an air-tight 1-L plastic container with 100 μL ethylene L^{-1} air or 10 μL L^{-1} 1-MCP generated by dissolving 48 mg of 1-MCP-releasing powder in 50 μL of water (Fujisawa et al., 2013). The treatment was conducted for 24 h in an incubator under 16 h of light and 8 h of dark at 25°C. After the treatment, the fruits were sliced, and seeds were removed, frozen in liquid nitrogen, and used for RNA isolation followed by RT-qPCR. At least three biological replicates were included for each treatment, and each replicate was from independent sampling.

TRV-Mediated VIGS in Tomato Fruit

The pTRV1 and pTRV2 VIGS vectors have been described previously (Liu et al., 2002). *A. tumefaciens* strain GV3101 containing pTRV1 or pTRV2 and its derivatives were used for the VIGS experiments. GV3101 containing the TRV-VIGS vectors was grown at 28°C in Luria-Bertani medium containing 10 mM MES (pH 5.6) and 20 mM acetosyringone with appropriate antibiotics (gentamicin and rifampicin for GV3101 and kanamycin for pTRV1 or pTRV2). After culturing overnight (28°C and 200 rpm), *A. tumefaciens* cells were harvested and resuspended in infiltration buffer (10 mM $MgCl_2$, 10 mM MES, pH 5.6, and 150 mM acetosyringone) to a final OD_{600} of 2 (for both pTRV1 or pTRV2 and its derivatives). *A. tumefaciens* containing pTRV1 and pTRV2 or the recombinant vectors were mixed in a 1:1 ratio and left for 11 h at room temperature before infiltration, as described previously (Fu et al., 2005). The tomato inflorescence peduncles attached to the fruit were injected with cultures of *A. tumefaciens* harboring the vectors using a 1-mL syringe. To detect the accumulation of virus and the silencing efficiency of specific genes in tomato fruit, RT-PCR and RT-qPCR were performed separately.

Color and Firmness Measurement

A hand-held colorimeter (CR-10 Plus) with the CIE L*a*b color system was chosen for pericarp color assay (Komatsu et al., 2016). The firmness of the pericarp was assayed using a hand-held penetrometer (model FT327 made in

Italy) according to the manufacturer's instructions. At least nine biological replicates were used for each assay, and each replicate was from independent sampling.

Carotenoid Content and Pathway Gene Expression Assay

Carotenoid extractions were performed as described previously (Fantini et al., 2013). Briefly, lyophilized tomato fruit powder was extracted with chloroform and methanol (2:1, v/v). Subsequently, 1 volume of 50 mM Tris buffer (pH 7.5, containing 1 M NaCl) was added, and the samples were kept for 20 min on ice. After centrifugation (15,000*g* for 10 min at 4°C), the organic phase was collected and reextracted. The combined organic phases for each sample were then dried by nitrogen blowing and resuspended in 100 μL of ethyl acetate. For each genotype, at least three independent extractions were performed. To identity and quantify the carotenoids, the Accurate-Mass HPLC1200/MS-QTOF 6520A (Agilent Technol) system packed with a reverse-phase column, 4.6 × 150 mm, 3 μm (YMC), was used, and the carotenoid was washed out by mobile phase A (81% methanol + 15% MTBE (methyl tert-butyl ether) + 4% water) and B (8% methanol + 90% MTBE + 2% water) at a flow rate 0.4 mL min^{-1}. Settings were as follows: DAD (diode array detection), 260 to 550 nm; mass range, 200 to 800; APCI (atmospheric pressure chemical ionization) ion source drying gas of N_2 at a pressure of 40 p.s.i., 350°C, 8 L min^{-1}; VCAP (voltage of capillary), 3,500 V; fragmentor, 160 V; skimmer, 65 V; OCT RF Vpp (OctPole radio frequency value of peak peak), 750 V; with the negative mass spectrometry scan mode 2GHzExt Dyn (3200). HPLC peak areas at 260 to 550 nm were integrated and calibrated by external standards (e.g. α-carotene, β-carotene, and lycopene; purchased from Sigma-Aldrich) mixed to generate multiple-diluted external calibration curves for quantification of the pigments. Carotenoids were identified based on typical retention times and specific published absorption spectra (Mialoundama et al., 2010; Régnier et al., 2015). DEGs in the carotenoid pathway were mapped using the MapMan database and visualized with colors representing the $\log_2$ fold change (Usadel et al., 2009; Jaiswal and Usadel, 2016).

Ethylene Production Measurement

For the measurement of ethylene production by fruit, each fruit was placed in a gas-tight 300-mL container at 25°C for 1 h, and a 1-mL headspace gas sample was analyzed using a gas chromatograph equipped with a flame ionization detector (Ma et al., 2016).

Statistical Analysis

Microsoft Excel 2010 and SPSS (SPSS Statistics, version 22) were used for statistical analyses. Data were subjected to ANOVA, and a comparison was carried out by Student's *t* test (*, $P < 0.05$ and **, $P < 0.01$). Duncan's multiple range test was used ($P < 0.05$).

Protein Extraction

Fruit proteins were isolated using the protocol described (Wang et al., 2006). Briefly, samples were ground into powder under liquid nitrogen, transferred to 2-mL tubes, which were filled with 10% TCA/acetone, mixed well, and centrifuged at 4°C, followed by removal of the supernatant, and the tubes were then topped up with 80% methanol and 0.1 M ammonium acetate. After centrifugation, the supernatant was discarded, the tubes were filled with 80% acetone, mixed well, and centrifuged, and the supernatant was again discarded and the samples air dried. Phenol (pH 8):SDS solution (30% Suc, 2% SDS, 0.2 M Tris, pH 8, and 5% β-mercaptoethanol [1:1, v/v]) was added to extract proteins, which were precipitated with 80% methanol and 0.1 M ammonium acetate, then the pellets were washed with 100% methanol and 80% acetone and finally dissolved in 2% SDS buffer (0.5 M Tris, pH 7, and 1.4% SDS).

Western Blotting

Protein extracts were separated on 10% SDS-PAGE gels and transferred to a polyvinylidene fluoride membrane. The membrane was blocked in 5% nonfat milk for 2 h at room temperature. Rabbit polyclonal or mouse monoclonal antibody was added at a ratio of 1:1,000 and incubated for 2 h at room temperature. Antibodies for protein tags (anti-myc and anti-HA) were from sigma (C3956 and H9658). Membranes were washed with Tris-buffered saline plus Tween 20 three times, 10 min each time. The anti-rabbit/anti-mouse horseradish peroxidase secondary antibody was added at a ratio of 1:10,000 and incubated for 2 h at room temperature. After three washes with Tris-buffered saline plus Tween 20, the membranes were visualized using a horseradish peroxidase-enhanced chemiluminescence system.

A. tumefaciens-Mediated Transient Expression in Planta

A. tumefaciens strain GV3101 (for BiFC and CoIP) or EHA105 (for trans-activation activity) containing recombinant vectors was used for transient expression assays. *A. tumefaciens* cells were cultured and harvested as described for the VIGS assay, and cells were resuspended to a final OD_{600} of 1 each. For BiFC, CoIP, and trans-activity assays, suspensions of the corresponding recombinant vectors were mixed in a 1:1 ratio, and the mixed suspension was infiltrated into *Nicotiana benthamiana* leaves using a 1-mL syringe without a needle. The fluorescence and luciferase activities were observed and measured at 2 to 5 d after infiltration.

Subcellular Localization

The CDS of target genes without the stop codon was amplified by PCR and subcloned into the pBI221-GFP vector, in frame with the GFP sequence. These fusion constructs and the control GFP vector were transformed into tobacco (*Nicotiana tabacum*) BY2 suspension culture cell protoplasts using the polyethylene glycol method (Shan et al., 2012; Ba et al., 2014). GFP fluorescence was observed with a fluorescence microscope (Zeiss7 10-3 channel). All transient expression assays were repeated at least three times.

Trans-Activation Assay

A dual luciferase trans-activity assay was performed as described by Ba et al. (2014) and Shan et al. (2014). The CDS of *RIN* or *RIN-MC* without stop codon was cloned into the pEAQ vector as effector (Sainsbury et al., 2009). Promoters of ripening-related genes were amplified by PCR, and the products were inserted into the pGreenII 0800-LUC double reporter vector fused to the LUC reporter gene; a REN luciferase under the control of the 35S promoter in the same vector was used as an internal control (Hellens et al., 2005). The constructed effector and reporter plasmids were transfected into *A. tumefaciens* strain EHA105 (pGreenII series holding psoup plasmid) separately and coinfected into *N. benthamiana* leaves. LUC/REN activities were measured using the dual luciferase assay kits (Promega) 2 to 5 d after infiltration. At least nine assay measurements were included for each assay.

BiFC Assay

Plasmids used were as described (Walter et al., 2004). The CDS of *RIN* or *RIN-MC* without stop codon was cloned into pSPYNE vector, and *FUL1*, *FUL2*, *MADS1*, and *TAGL1* were cloned into pSPYCE vector and transfected into *A. tumefaciens* strain GV3101 separately, using protocols for *A. tumefaciens*-mediated transient expression in infiltrated leaves (Piotrzkowski et al., 2012). The fluorescence was observed at 2 to 5 d after infiltration.

CoIP Assay

The CDS of *RIN* or *RIN-MC* without stop codon was fused with 6myc tags and cloned into pCAMBIA1300-221 vector, and *FUL1*, *FUL2*, *MADS1*, and *TAGL1* were fused with 3HA tags. Recombinant vectors were transfected into *A. tumefaciens* strain GV3101 separately, using protocols for *A. tumefaciens*-mediated transient expression in infiltrated leaves. The assay procedures were as described (Kim et al., 2009; Deng et al., 2014). *N. benthamiana* leaves were ground in liquid nitrogen, and proteins were extracted with extraction buffer (20 mM HEPES-KOH, pH 7.5, 40 mM KCl, 1 mM EDTA, 0.5% Triton X-100, and 1× protease inhibitors; Roche) at a ratio of 3 mL g^{-1} tissue powder. After 10 min of centrifugation at 20,000*g*, the supernatant was incubated with anti-myc agarose (Sigma-Aldrich) for 1 h. The retained proteins on beads were then washed four times with wash buffer (20 mM HEPES-KOH, pH 7.5, 40 mM KCl, and 0.01% Triton X-100), eluted by boiling in 2× SDS sample buffer for 10 min, and analyzed on protein blots after gel electrophoresis using anti-myc or anti-HA antibody (Sigma-Aldrich).

RNA Sequencing and Bioinformatics Assay

Total RNA samples were prepared from tomato fruits of the wild type (AC), *rin* mutants, and transgenic AC *35S::RIN* RNAi and *rin 35S::RIN-MC* RNAi at BK+5 (three replicates per sample). The extraction and quality control of total RNA and DNA digestion were as described above. The pair-end sequencing was performed on an Illumina HiSeq2500 PE150 by Novogene, generating at least 6 G of raw data. Raw data were pretreated using FASTX-Toolkit (version

0.0.13.2; http://hannonlab.cshl.edu/fastx_toolkit/download.html), and the resulting clean reads were checked for quality using the Q < 20 threshold and aligned with the tomato reference genome using TopHat (version 2.0.8; http://ccb.jhu.edu/software/tophat/index.shtml). Reads with less than two mismatches were used to construct transcripts using Cufflinks (version 2.0.2; http://cole-trapnell-lab.github.io/cufflinks/). All clean reads were deposited in the National Center for Biotechnology Information Sequence Read Archive (http://www.ncbi.nlm.nih.gov/sra/) under the accession numbers SRP106816 (data in VIGS assay) and SRP106775 (data in *RIN* and *RIN-MC*-suppressed assay). Genes were considered as DEGs under the threshold of $\log_2$ fold change ≥ 1, $q < 0.05$, and FPKM > 10 in either sample. A heat map was plotted to visualize gene expression using the pheatmap package (Dailey, 2017).

GO Enrichment Analysis

GO enrichment analysis was performed using BiNGO (Maere et al., 2005) based on DEGs, using threshold values of $P < 0.05$ and FPKM > 10 for each sample. Genes were classified into three classes: cellular component, biological process, and molecular function.

KEGG Pathway Enrichment Analysis

Fasta format files containing DEG protein sequences were obtained using in-house Perl scripts, and KEGG enrichment analysis was then performed in KOBAS (version 2.0; http://obas.cbi.pku.edu.cn/download.do), based on native BLAST tools and organism annotation libraries. KEGG pathways with $P < 0.05$ and FPKM > 10 for each sample were analyzed and visualized with R Project (R version 3.4.0; https://www.r-project.org/).

Accession Numbers

Sequence data from this article can be found in the GenBank/EMBL data libraries under accession numbers SRP106816 (data in VIGS assay) and SRP106775 (data in RIN and RIN-MC-suppressed assay).

Supplemental Data

The following supplemental materials are available.

Supplemental Figure S1. Primer design and virus detection of VIGS in tomato fruits.

Supplemental Figure S2. Transcriptome assay of ripening genes in *RIN-MC*-silenced tomato fruits.

Supplemental Figure S3. Photographs of four kinds of tomato fruits at different ripening stages.

Supplemental Figure S4. Expression of genes involved in coloring during ripening of four kinds of tomato fruits.

Supplemental Figure S5. Physiological traits of four kinds of tomato fruits at different ripening stages.

Supplemental Figure S6. Comparison of DEGs in two kinds of tomato fruits.

Supplemental Figure S7. Comparison of DEGs in AC/AC *35S*::*RIN* RNAi and *rin*/*rin* *35S*::*RIN-MC* RNAi.

Supplemental Figure S8. Trans-activities of tomato RIN and RIN-MC using different lengths of *RIN* promoters in a transient in planta expression system.

Supplemental Figure S9. Trans-activation activities of tomato RIN and RIN-MC with different lengths of *RIN* promoters in a transient in planta expression system.

Supplemental Tables S1 and S2. Sequences of all the primers designed.

Supplemental Data Sets S1 to S3. RNA sequencing data.

Supplemental Data Sets S4 to S11. List of DEGs regulated by RIN or RIN-MC that exist in different regions in the Venn diagram.

Supplemental Data Sets S12 and S13. List of DEGs regulated by RIN or RIN-MC that are enriched in the GO enrichment assay (Supplemental Fig. S7A).

Supplemental Data Sets S14 and S15. List of DEGs regulated by RIN or RIN-MC that are enriched in the KEGG assay.

ACKNOWLEDGMENTS

We thank Jianye Chen and Dr. Jianfei Kuang (South China Agricultural University) for the generous gift of tobacco BY2 suspension cells and pGreenII 0800 series vectors; Xian Li (Zhejiang University) for help with experimental technique; Zhipeng Deng (Zhejiang Academy of Agricultural Science) for help with article revision; and the Institute of Plant Physiology and Ecology, Shanghai institutes for biological sciences (SIBS) Chinese Academy of Sciences, for carotenoid content detection.

Received October 10, 2017; accepted November 9, 2017; published November 13, 2017.

LITERATURE CITED

Alba R, Payton P, Fei Z, McQuinn R, Debbie P, Martin GB, Tanksley SD, Giovannoni JJ (2005) Transcriptome and selected metabolite analyses reveal multiple points of ethylene control during tomato fruit development. Plant Cell **17:** 2954–2965

Annala MJ, Parker BC, Zhang W, Nykter M (2013) Fusion genes and their discovery using high throughput sequencing. Cancer Lett **340:** 192–200

Ba L, Shan W, Kuang J, Feng B, Xiao Y, Lu W, Chen J (2014) The banana MaLBD (LATERAL ORGAN BOUNDARIES DOMAIN) transcription factors regulate EXPANSIN expression and are involved in fruit ripening. Plant Mol Biol Rep **32:** 1103–1113

Barry CS, Giovannoni JJ (2007) Ethylene and fruit ripening. J Plant Growth Regul **26:** 143–159

Boycheva S, Daviet L, Wolfender JL, Fitzpatrick TB (2014) The rise of operon-like gene clusters in plants. Trends Plant Sci **19:** 447–459

Chen G, Hackett R, Walker D, Taylor A, Lin Z, Grierson D (2004) Identification of a specific isoform of tomato lipoxygenase (TomloxC) involved in the generation of fatty acid-derived flavor compounds. Plant Physiol **136:** 2641–2651

Chiarle R, Voena C, Ambrogio C, Piva R, Inghirami G (2008) The anaplastic lymphoma kinase in the pathogenesis of cancer. Nat Rev Cancer **8:** 11–23

DellaPenna D, Lincoln JE, Fischer RL, Bennett AB (1989) Transcriptional analysis of polygalacturonase and other ripening associated genes in Rutgers, rin, nor, and Nr tomato fruit. Plant Physiol **90:** 1372–1377

Deng Z, Oses-Prieto JA, Kutschera U, Tseng TS, Hao L, Burlingame AL, Wang ZY, Briggs WR (2014) Blue light-induced proteomic changes in etiolated Arabidopsis seedlings. J Proteome Res **13:** 2524–2533

Dong T, Hu Z, Deng L, Wang Y, Zhu M, Zhang J, Chen G (2013) A tomato MADS-box transcription factor, SlMADS1, acts as a negative regulator of fruit ripening. Plant Physiol **163:** 1026–1036

Enfissi EMA, Nogueira M, Bramley PM, Fraser PD (2017) The regulation of carotenoid formation in tomato fruit. Plant J **89:** 774–788

Fantini E, Falcone G, Frusciante S, Giliberto L, Giuliano G (2013) Dissection of tomato lycopene biosynthesis through virus-induced gene silencing. Plant Physiol **163:** 986–998

Fray RG, Grierson D (1993) Identification and genetic analysis of normal and mutant phytoene synthase genes of tomato by sequencing, complementation and co-suppression. Plant Mol Biol **22:** 589–602

Fu DQ, Zhu BZ, Zhu HL, Jiang WB, Luo YB (2005) Virus-induced gene silencing in tomato fruit. Plant J **43:** 299–308

Fujisawa M, Nakano T, Shima Y, Ito Y (2013) A large-scale identification of direct targets of the tomato MADS box transcription factor RIPENING INHIBITOR reveals the regulation of fruit ripening. Plant Cell **25:** 371–386

Fujisawa M, Shima Y, Higuchi N, Nakano T, Koyama Y, Kasumi T, Ito Y (2012) Direct targets of the tomato-ripening regulator RIN identified by transcriptome and chromatin immunoprecipitation analyses. Planta **235:** 1107–1122

Fujisawa M, Shima Y, Nakagawa H, Kitagawa M, Kimbara J, Nakano T, Kasumi T, Ito Y (2014) Transcriptional regulation of fruit ripening by tomato FRUITFULL homologs and associated MADS box proteins. Plant Cell **26:** 89–101

Giovannoni JJ (2004) Genetic regulation of fruit development and ripening. Plant Cell **(Suppl) 16:** S170–S180

Grierson D (2013) Ethylene and the control of fruit ripening. *In* GB Seymour, M Poole, JJ Giovannoni, GA Tucker, eds, The Molecular Biology and Biochemistry of Fruit Ripening. Blackwell Publishing, Oxford, doi/10.1002/9781118593714.ch3

Hagel JM, Facchini PJ (2017) Tying the knot: occurrence and possible significance of gene fusions in plant metabolism and beyond. J Exp Bot **68:** 4029–4043

Hellens RP, Allan AC, Friel EN, Bolitho K, Grafton K, Templeton MD, Karunairetnam S, Gleave AP, Laing WA (2005) Transient expression vectors for functional genomics, quantification of promoter activity and RNA silencing in plants. Plant Methods **1:** 13

Itkin M, Seybold H, Breitel D, Rogachev I, Meir S, Aharoni A (2009) TOMATO AGAMOUS-LIKE 1 is a component of the fruit ripening regulatory network. Plant J **60:** 1081–1095

Ito Y, Kitagawa M, Ihashi N, Yabe K, Kimbara J, Yasuda J, Ito H, Inakuma T, Hiroi S, Kasumi T (2008) DNA-binding specificity, transcriptional activation potential, and the *rin* mutation effect for the tomato fruit-ripening regulator RIN. Plant J **55:** 212–223

Ito Y, Nishizawa-Yokoi A, Endo M, Mikami M, Shima Y, Nakamura N, Kotake-Nara E, Kawasaki S, Toki S (2017) Re-evaluation of the rin mutation and the role of RIN in the induction of tomato ripening. Nat Plants **3:** 866–874

Ito Y, Nishizawa-Yokoi A, Endo M, Mikami M, Toki S (2015) CRISPR/Cas9-mediated mutagenesis of the RIN locus that regulates tomato fruit ripening. Biochem Biophys Res Commun **467:** 76–82

Jaiswal P, Usadel B (2016) Plant pathway databases. Methods Mol Biol **1374:** 71–87

Karlova R, Rosin FM, Busscher-Lange J, Parapunova V, Do PT, Fernie AR, Fraser PD, Baxter C, Angenent GC, de Maagd RA (2011) Transcriptome and metabolite profiling show that APETALA2a is a major regulator of tomato fruit ripening. Plant Cell **23:** 923–941

Kaufmann K, Melzer R, Theissen G (2005) MIKC-type MADS-domain proteins: structural modularity, protein interactions and network evolution in land plants. Gene **347:** 183–198

Kim TW, Guan S, Sun Y, Deng Z, Tang W, Shang JX, Sun Y, Burlingame AL, Wang ZY (2009) Brassinosteroid signal transduction from cell-surface receptor kinases to nuclear transcription factors. Nat Cell Biol **11:** 1254–1260

Kimura S, Sinha N (2008) Tomato transformation. CSH Protoc **2008:** t5084

Klee HJ, Giovannoni JJ (2011) Genetics and control of tomato fruit ripening and quality attributes. Annu Rev Genet **45:** 41–59

Komatsu T, Mohammadi S, Busa LS, Maeki M, Ishida A, Tani H, Tokeshi M (2016) Image analysis for a microfluidic paper-based analytical device using the CIE L*a*b* color system. Analyst (Lond) **141:** 6507–6509

Li J, Lee EJ, Chang L, Facchini PJ (2016) Genes encoding norcoclaurine synthase occur as tandem fusions in the Papaveraceae. Sci Rep **6:** 39256

Liu M, Gomes BL, Mila I, Purgatto E, Peres LEP, Frasse P, Maza E, Zouine M, Roustan JP, Bouzayen M, et al (2016) Comprehensive profiling of ethylene response factor expression identifies ripening-associated *ERF* genes and their link to key regulators of fruit ripening in tomato. Plant Physiol **170:** 1732–1744

Liu Y, Schiff M, Dinesh-Kumar SP (2002) Virus-induced gene silencing in tomato. Plant J **31:** 777–786

Livak KJ, Schmittgen TD (2001) Analysis of relative gene expression data using real-time quantitative PCR and the 2(-Delta Delta C(T)) method. Methods **25:** 402–408

Long M, Betrán E, Thornton K, Wang W (2003) The origin of new genes: glimpses from the young and old. Nat Rev Genet **4:** 865–875

Luo Z, Zhang J, Li J, Yang C, Wang T, Ouyang B, Li H, Giovannoni J, Ye Z (2013) A STAY-GREEN protein SlSGR1 regulates lycopene and β-carotene accumulation by interacting directly with SlPSY1 during ripening processes in tomato. New Phytol **198:** 442–452

Ma Y, Zhou L, Wang Z, Chen J, Qu G (2016) Oligogalacturonic acids promote tomato fruit ripening through the regulation of 1-aminocyclopropane-1-carboxylic acid synthesis at the transcriptional and post-translational levels. BMC Plant Biol **16:** 13

Maere S, Heymans K, Kuiper M (2005) BiNGO: a Cytoscape plugin to assess overrepresentation of Gene Ontology categories in biological networks. Bioinformatics **21:** 3448–3449

Manning K, Tör M, Poole M, Hong Y, Thompson AJ, King GJ, Giovannoni JJ, Seymour GB (2006) A naturally occurring epigenetic mutation in a gene encoding an SBP-box transcription factor inhibits tomato fruit ripening. Nat Genet **38:** 948–952

Martel C, Vrebalov J, Tafelmeyer P, Giovannoni JJ (2011) The tomato MADS-box transcription factor RIPENING INHIBITOR interacts with promoters involved in numerous ripening processes in a COLORLESS NONRIPENING-dependent manner. Plant Physiol **157:** 1568–1579

Matas AJ, Gapper NE, Chung MY, Giovannoni JJ, Rose JK (2009) Biology and genetic engineering of fruit maturation for enhanced quality and shelf-life. Curr Opin Biotechnol **20:** 197–203

McWhirter JR, Galasso DL, Wang JY (1993) A coiled-coil oligomerization domain of Bcr is essential for the transforming function of Bcr-Abl oncoproteins. Mol Cell Biol **13:** 7587–7595

Mellidou I, Chagné D, Laing WA, Keulemans J, Davey MW (2012) Allelic variation in paralogs of GDP-L-galactose phosphorylase is a major determinant of vitamin C concentrations in apple fruit. Plant Physiol **160:** 1613–1629

Mialoundama AS, Heintz D, Jadid N, Nkeng P, Rahier A, Deli J, Camara B, Bouvier F (2010) Characterization of plant carotenoid cyclases as members of the flavoprotein family functioning with no net redox change. Plant Physiol **153:** 970–979

Mitelman F, Johansson B, Mertens F (2007) The impact of translocations and gene fusions on cancer causation. Nat Rev Cancer **7:** 233–245

Nützmann HW, Osbourn A (2014) Gene clustering in plant specialized metabolism. Curr Opin Biotechnol **26:** 91–99

Ohta M, Matsui K, Hiratsu K, Shinshi H, Ohme-Takagi M (2001) Repression domains of class II ERF transcriptional repressors share an essential motif for active repression. Plant Cell **13:** 1959–1968

Osorio S, Alba R, Damasceno CM, Lopez-Casado G, Lohse M, Zanor MI, Tohge T, Usadel B, Rose JK, Fei Z, Giovannoni JJ, Fernie AR (2011) Systems biology of tomato fruit development: combined transcript, protein, and metabolite analysis of tomato transcription factor (nor, rin) and ethylene receptor (Nr) mutants reveals novel regulatory interactions. Plant Physiol **157:** 405–425

Piotrzkowski N, Schillberg S, Rasche S (2012) Tackling heterogeneity: a leaf disc-based assay for the high-throughput screening of transient gene expression in tobacco. PLoS One **7:** e45803

Qin G, Wang Y, Cao B, Wang W, Tian S (2012) Unraveling the regulatory network of the MADS box transcription factor RIN in fruit ripening. Plant J **70:** 243–255

Régnier P, Bastias J, Rodriguez-Ruiz V, Caballero-Casero N, Caballo C, Sicilia D, Fuentes A, Maire M, Crepin M, Letourneur D, et al (2015) Astaxanthin from Haematococcus pluvialis prevents oxidative stress on human endothelial cells without toxicity. Mar Drugs **13:** 2857–2874

Ren J, Wen L, Gao X, Jin C, Xue Y, Yao X (2009) DOG 1.0: illustrator of protein domain structures. Cell Res **19:** 271–273

Sainsbury F, Thuenemann EC, Lomonossoff GP (2009) pEAQ: versatile expression vectors for easy and quick transient expression of heterologous proteins in plants. Plant Biotechnol J **7:** 682–693

Sakuraba Y, Park SY, Paek NC (2015) The divergent roles of STAYGREEN (SGR) homologs in chlorophyll degradation. Mol Cells **38:** 390–395

Seymour G, Poole M, Manning K, King GJ (2008) Genetics and epigenetics of fruit development and ripening. Curr Opin Plant Biol **11:** 58–63

Shahmuradov IA, Abdulazimova AU, Solovyev VV, Qamar R, Cholan SN, Aliyev JA (2010) Mono- and bi-cistronic chimeric mRNAs in Arabidopsis and rice genomes. Appl Comput Math **9:** 66–81

Shan W, Kuang JF, Chen L, Xie H, Peng HH, Xiao YY, Li XP, Chen WX, He QG, Chen JY, et al (2012) Molecular characterization of banana NAC transcription factors and their interactions with ethylene signalling component EIL during fruit ripening. J Exp Bot **63:** 5171–5187

Shan W, Kuang JF, Lu WJ, Chen JY (2014) Banana fruit NAC transcription factor MaNAC1 is a direct target of MaICE1 and involved in cold stress through interacting with MaCBF1. Plant Cell Environ **37:** 2116–2127

Shima Y, Kitagawa M, Fujisawa M, Nakano T, Kato H, Kimbara J, Kasumi T, Ito Y (2013) Tomato FRUITFULL homologues act in fruit ripening via forming MADS-box transcription factor complexes with RIN. Plant Mol Biol **82:** 427–438

Singh D, Chan JM, Zoppoli P, Niola F, Sullivan R, Castano A, Liu EM, Reichel J, Porrati P, Pellegatta S, et al (2012) Transforming fusions of FGFR and TACC genes in human glioblastoma. Science **337:** 1231–1235

Sun HJ, Uchii S, Watanabe S, Ezura H (2006) A highly efficient transformation protocol for Micro-Tom, a model cultivar for tomato functional genomics. Plant Cell Physiol **47:** 426–431

Tomato Genome Consortium (2012) The tomato genome sequence provides insights into fleshy fruit evolution. Nature **485:** 635–641

Usadel B, Poree F, Nagel A, Lohse M, Czedik-Eysenberg A, Stitt M (2009) A guide to using MapMan to visualize and compare omics data in

plants: a case study in the crop species, maize. Plant Cell Environ **32:** 1211–1229

Vrebalov J, Ruezinsky D, Padmanabhan V, White R, Medrano D, Drake R, Schuch W, Giovannoni J (2002) A MADS-box gene necessary for fruit ripening at the tomato ripening-inhibitor (rin) locus. Science **296:** 343–346

Walter M, Chaban C, Schütze K, Batistic O, Weckermann K, Näke C, Blazevic D, Grefen C, Schumacher K, Oecking C, et al (2004) Visualization of protein interactions in living plant cells using bimolecular fluorescence complementation. Plant J **40:** 428–438

Wang W, Vignani R, Scali M, Cresti M (2006) A universal and rapid protocol for protein extraction from recalcitrant plant tissues for proteomic analysis. Electrophoresis **27:** 2782–2786

Yu J, Tehrim S, Wang L, Dossa K, Zhang X, Ke T, Liao B (2017) Evolutionary history and functional divergence of the cytochrome P450 gene superfamily between Arabidopsis thaliana and Brassica species uncover effects of whole genome and tandem duplications. BMC Genomics **18:** 733

Zhong S, Fei Z, Chen YR, Zheng Y, Huang M, Vrebalov J, McQuinn R, Gapper N, Liu B, Xiang J, et al (2013) Single-base resolution methylomes of tomato fruit development reveal epigenome modifications associated with ripening. Nat Biotechnol **31:** 154–159

Zhu B, Yang Y, Li R, Fu D, Wen L, Luo Y, Zhu H (2015) RNA sequencing and functional analysis implicate the regulatory role of long non-coding RNAs in tomato fruit ripening. J Exp Bot **66:** 4483–4495

Zi J, Mafu S, Peters RJ (2014) To gibberellins and beyond! Surveying the evolution of (di)terpenoid metabolism. Annu Rev Plant Biol **65:** 259–286